Failure and Degradation Modes of PV modules in a Hot Dry Climate:

Results after 16 years of field exposure

by

Karan Rao Yedidi

A Thesis Presented in Partial Fulfillment
of the Requirements for the Degree
Master of Science in Technology

Approved November 2013 by the
Graduate Supervisory Committee

Govindasamy Tamizhmani, Chair
Devarajan Srinivasan
Narciso Macia

ARIZONA STATE UNIVERSITY

December 2013

ABSTRACT

This study evaluates two 16 year old photovoltaic power (PV) plants to ascertain degradation rates and various failure modes which occur in a “hot-dry” climate. The data obtained from this study can be used by module manufacturers in determining the warranty limits of their modules and also by banks, investors, project developers and users in determining appropriate financing or decommissioning models. In addition, the data obtained in this study will be helpful in selecting appropriate accelerated stress tests which would replicate the field failures for the new modules and would predict the lifetime for new PV modules. The two power plants referred to as Site 4A and -4B with (1512 modules each) were initially installed on a single axis tracking system in Gilbert, Arizona for the first seven years and have been operating at their current location in Mesa, Arizona for the last nine years at fixed horizontal tilt Both sites experience hot-dry desert climate. Average degradation rate is 0.85%/year for the best modules and 1.1%/year for all the modules (excluding the safety failed modules). Primary safety failure mode is the backsheet delamination though it is small (less than 1.7%). Primary degradation mode and reliability failure mode may potentially be attributed to encapsulant browning leading to transmittance/current loss and thermo-mechanical solder bond fatigue (cell-ribbon and ribbon-ribbon) leading to series resistance increase. Average soiling loss of horizontal tilt based modules is 11.1%. About 0.5-1.7% of the modules qualify for the safety returns under the typical 20/20 warranty terms, 73-76% of the modules qualify for the warranty claims under the typical 20/20 power warranty terms and 24-26% of the modules are meeting the typical 20/20 power warranty terms.

DEDICATION

I would like to dedicate this thesis to my parents and my sister, for their support throughout my master's study. Without their love and support, none of this would be possible.

ACKNOWLEDGMENTS

I would like to thank Dr.Govindasamy TamizhMani for his constant guidance and support throughout the project. I would also like to thank Dr. Narcisco Macia and Dr.Devarajan Srinivasan for readily accepting to be on my advising committee.

I would like to thank Mr. Joseph Kuitche for giving me the opportunity to work at Arizona State University Photovoltaic Reliability Laboratory and involve me with these great projects. I gained great knowledge while working under his supervision at PRL.

Thanks to SRP (Salt River Project) for their support to execute the project successfully. I would like to thank Mr. Bill Kazesta for the knowledge he shared with me. My appreciation goes to Brent Schuster, Hannoush Eric, and Dan Wilson for their support during the testing. I appreciate the joint working partnership with Jaya Krishna Mallineni on this project.

I ‘am grateful to Brett Knisely and Sai Tatapudi for their thorough field support and motivation through the course of my project.

I would also like to thank my friends Cameron Anderson, Kolapo Olakonu, Suryanarayana Vasantha Janakeeraman, Sanjay Mohan Shrestha and Shikha Rawat for their support and advice.

TABLE OF CONTENTS

Page

CHAPTER Page

CHAPTER Page

LIST OF TABLES

LIST OF FIGURES

Figure Page

Figure Page

Figure Page

LIST OF VARIABLES

A= Current in Amperes

In^2 = Square Inches

W/m^2= Watts / $Meter^2$

kW = Kilowatts

Isc = Short Circuit Current

V_{oc} = Voltage Open Circuit

Imax= Maximum Current

Vmax= Maximum Voltage

FF = Fill Factor

STC = Standard Test Conditions (25^oC, 1000 W/m^2)

CHAPTER 1

INTRODUCTION

1.1 Background

Approximately 10-years ago, Salt River Project (SRP) installed three photovoltaic systems (Site 4A, Site 4B, and Site 4C) in Mesa as part of its Earth-Wise™ Energy Program. This program allows customers to purchase electricity generated from renewable energy sources.

Figure 1 Site-4A&4B, Mesa, AZ [1]

The PV systems in Phase 1 (Site 4A) and Phase 2 (Site 4B) use a total of 3,024 monocrystalline silicon frameless PV modules, which cover an area of approximately 20,617 square feet. These systems are 16-years-old, installed horizontally, and fixed in place. The DC power generated by the two PV systems is converted to alternating current by a SMA Sunny Central 125 kW inverter [1].

Since the modules have many years of operation, information on their durability and reliability issues can help predict the useful life of modules used in newer power plants. The results of this study along with the results of other similar studies can be used to better predict the useful life of modules in "hot-dry" desert climatic conditions.

1.2 Objective

The objective of this study is to evaluate 3,024 solar PV modules that were deployed 16-years ago. This study was conducted to identify the major PV durability and reliability issues that are contributing to power loss at a string level as well at a module level. The main focus of this study is to substantiate 5 primary results:

1. To calculate the degradation rates of modules and strings
2. To obtain evidence confirming the absence/presence of potential induced degradation (PID).
3. To highlight the durability and reliability issues particular to "hot-dry" climate.
4. To highlight the losses in soiling due to a horizontally fixed tracking system.
5. To look for effects of wind direction on performance degradation.

The results of this study will be beneficial to the PV industry since it will: allow researchers to design appropriate accelerated tests for newer modules; enable manufacturers to make better material choices for construction of modules; and assist financial communities to determine long-term PV profitability.

1.3 Scope of Project

The following flowchart shows an outline of all the tests that were performed as a part of this power plant evaluation. The tests performed on site are:

- 144 soiled string level I-V measurements
- 42 cleaned individual modules I-V measurements
- Visual Inspection, IR imaging and diode check of all 1512 modules.

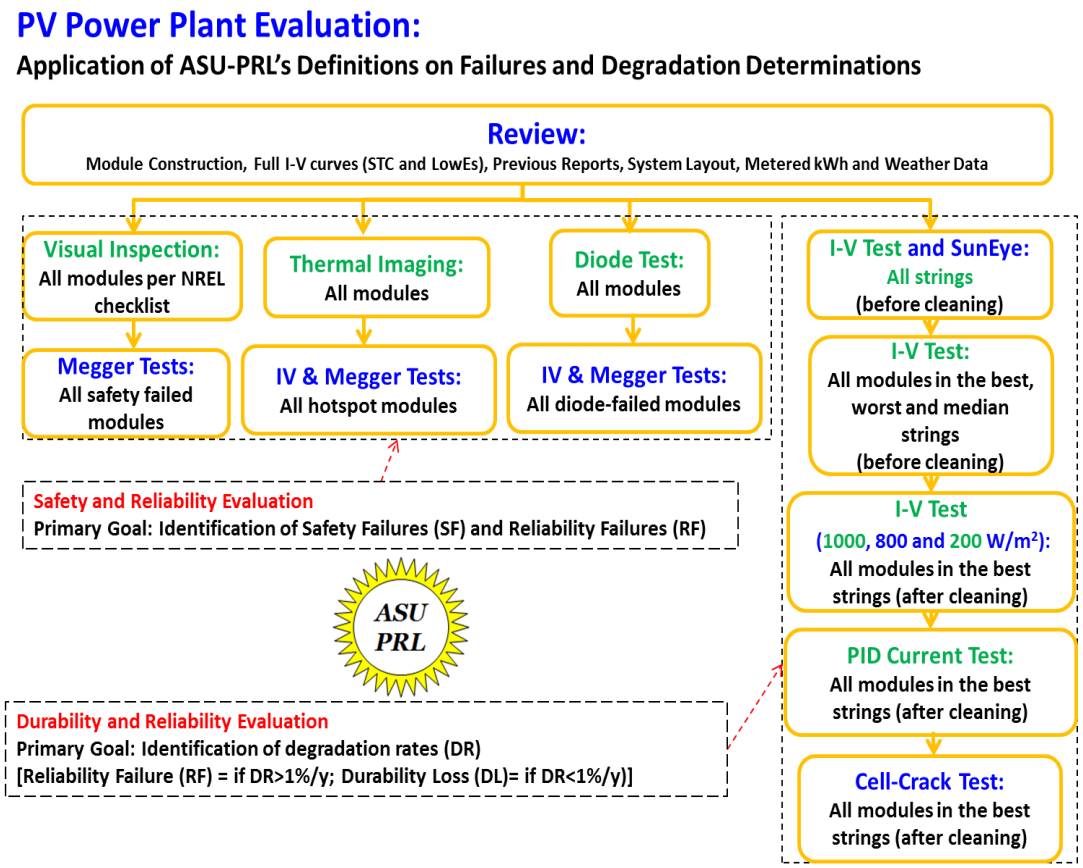

Figure 2 Tests Performed

CHAPTER 2

LITERATURE REVIEW

2.1 Need for Reliability and lifetime prediction

The reliability and lifespan of PV modules depends heavily upon module construction and the climate in which it is installed [2]. In today's market, large scale PV investors routinely analyze the technology risk while focusing on reliability and durability issues. This is done to realize the return on investment (ROI) in the case of investors, and levelized cost of energy (LCOE, $/kWh) in the case of utility companies. In recent years, manufacturers offer warranties up to 25 years or more on their modules. Currently, little can be said about the effectiveness of these warranties, as most manufacturers have left the industry due to growing global competition. Numerous PV power plants have been established around the world, utilizing hundreds of thousands of these modules from now defunct manufacturers.

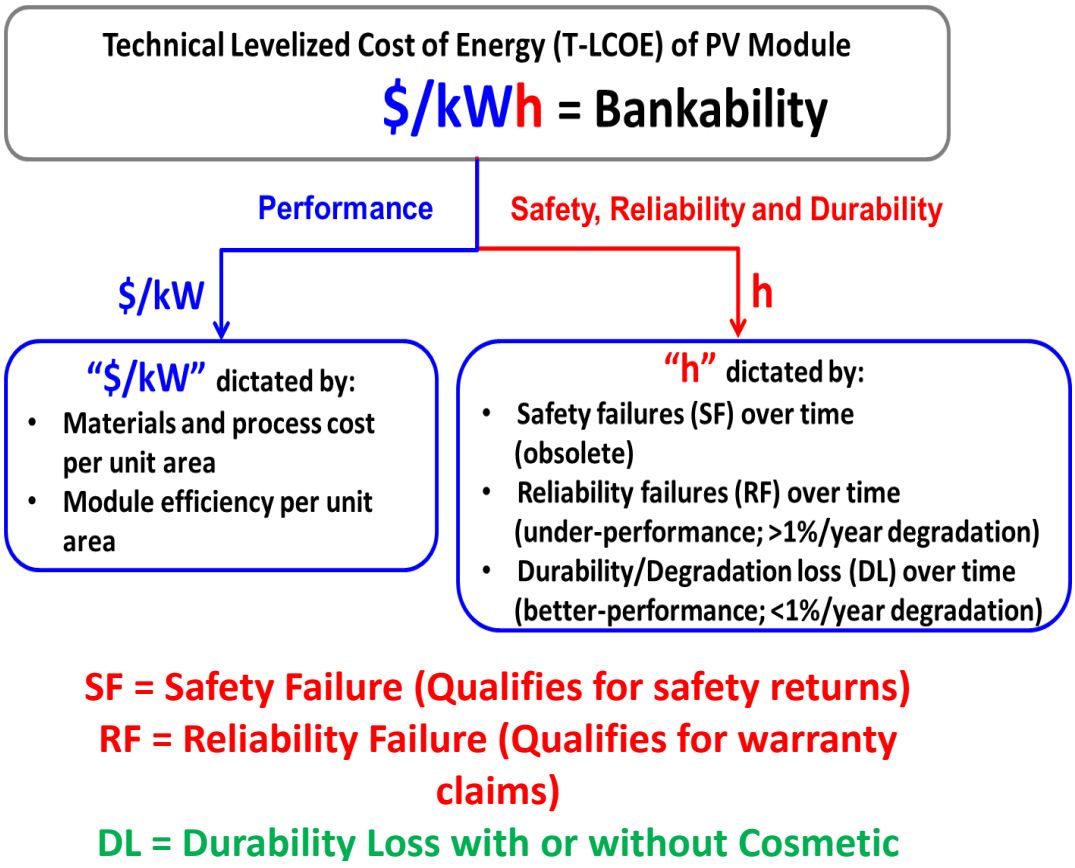

Figure 3 Goal of the PV industry [3]

2.2 Reliability and durability of PV modules:

Reliability: If the PV modules are removed (or replaced) from the field before the warranty period expires due to any type of failure, including power drop beyond the warranty limit, then those failures are classified as hard failures [3].

Durability: If the performance of PV modules degrades but still meets the warranty requirements, then those losses may be classified as soft losses or degradative losses [3].

Towards a module's end-of-life, multiple degradative mechanisms may develop and lead to wear-out failures due to accelerated degradative losses. Durability issues could be attributed to the materials used for manufacturing PV modules [3]. Reliability failures are catastrophic failures which could be attributed to the design and production issues.

Numerous studies have been conducted on multiple power plants to identify and understand the different failure modes and mechanisms effecting modules exposed in the field. Once the failure modes and mechanisms are identified, they can be simulated in a controlled environment. This method of simulating field like conditions at an accelerated pace in a controlled laboratory environment is called accelerated testing. This type of testing stresses a module for a certain period of time (acceleration factor) and provides valuable information regarding how long the module will last in the field. A typical manufacturer's 20 year warranty guarantees its module to a point where if the Power > or = 80% of minimum rated power, the module is good and within warrantee.

The failure or degradation modes in PV modules indicate symptoms, whereas failure or degradation mechanisms represent the course for arriving at these symptoms. Field failures and degradation losses may be classified as reliability failures and durability losses, respectively [3].

2.3 Bathtub curve

The failures that occur in the infant mortality stage are mostly due to quality and design issues, the region in the middle is considered as the useful life of the module, catastrophic failures are relatively lower in this region when compared to the beginning or the end of life, issues in the useful life of modules may be attributed to production quality issues. The final region is the end of life of modules where failures rates can increase and the modules end up producing less than 80% of their rated power, at which point in time, it makes more sense to decommission them [3].

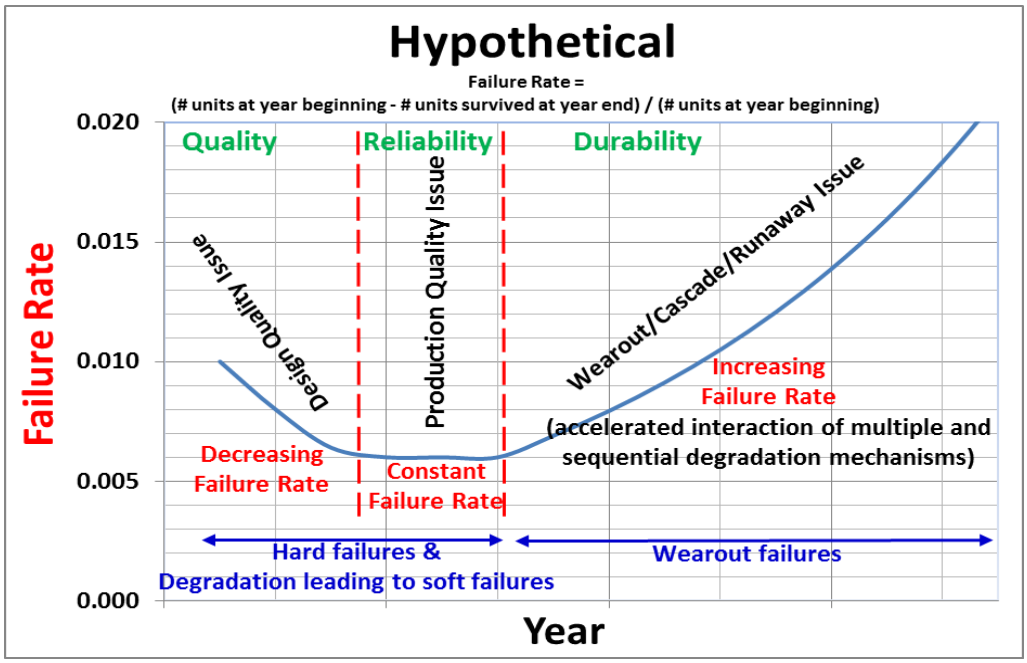

Figure 4 Bathtub Curve (Hypothetical) [3]

2.4 Failure Mechanisms and Failure Modes

A failure mechanism is responsible for one or more failure modes. A failure mechanism could be triggered by one or more failure causes and a failure mode could trigger one or more failure effects [3]. The field failure analysis approach for PV modules may be represented as shown in the following sequence

Failure Mechanism (Cause) → Failure Mode (Effect)

Example:

Thermo-mechanical fatigue (Expansions-Contractions) → Broken interconnects (Arcing)

Broken interconnects, solder bond failures, hotspots, encapsulant delamination, back sheet warping are examples of failure modes. Thermal expansion and contraction can be considered the major cause for broken interconnects and solder bond failures. Encapsulant delamination is caused by the sensitivity of adhesive bonds to ultra violet light at high temperatures or to humidity in field. Encapsulant delamination can also be caused by contamination from material (Excess Na in glass or acetic acid from encapsulant). Hot spots are mainly caused by shadowing, faulty cells, low shunt resistance, and failure of bypass diodes. Degradation Modes includes slow corrosion, gradual encapsulant discoloration, and back sheet detaching/cracking/warping. Gradual encapsulant discoloration can be caused by UV exposure at higher operating temperatures, reduced breathability, and/or inappropriate additives in EVA [3]. The major degradation modes found in “hot-dry” climates are solder bond deterioration and encapsulant discoloration.

2.5 Solder Bond Fatigue

The mechanical and electrical quality of solar cell interconnection ribbon bonds is critical in optimizing photovoltaic manufacturing yield, energy conversion efficiency, and product life expectancy. During the soldering process, a significant differential in the thermal coefficient of expansion (TCE) between the copper ribbon and polysilicon takes place when processing temperatures are greater than 300ºC and above. This differential applies stresses to the substrate which can result in the formation of micro-cracks that may not be detected during the manufacturing process, and can result in a less than expected in-field product life span [4]. The ribbon wire is made of copper metal and soldered by SnPbAg as shown in Figure 5. The ribbon carries the current from each solar cell to the junction box. The main cause for solder bond cracks is the mismatch of the thermal expansion coefficient between the module material and ribbon wire solder. Solder bond fatigue/failure occurs mostly due to the following factors:

- Thermal expansion and contraction.
- Poor quality of solder bond process
- Flexing due to wind loading
- Vibration due to packing and transportation.

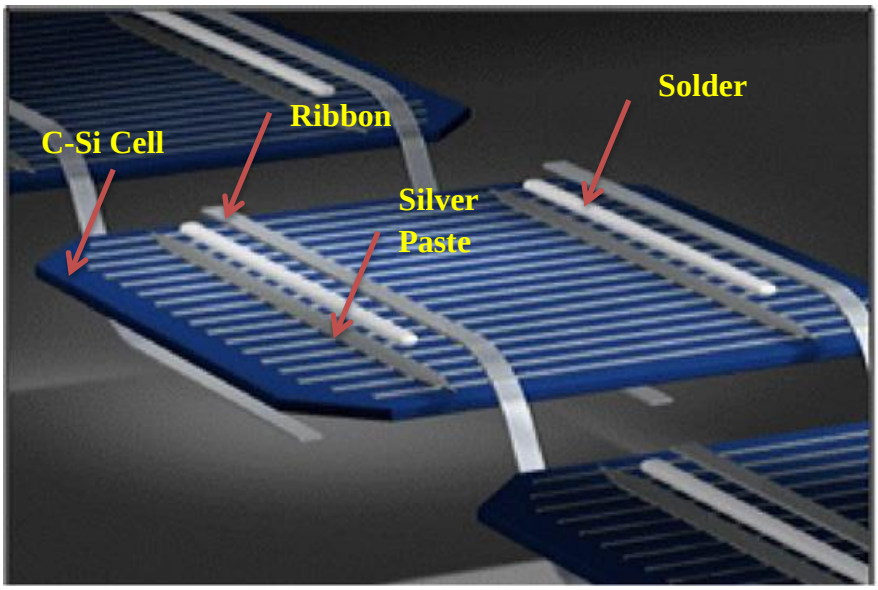

Figure 5 Solder interconnection between ribbon wire and silicon solar cell [4]

2.6 Encapsulant Discoloration:

Photovoltaic (PV) devices are typically encapsulated using ethylene-vinyl acetate (EVA) to provide mechanical support, electrical isolation, and protection against environmental exposure. Under exposure to water and/or ultraviolet radiation, EVA will decompose to produce acetic acid that will lower the pH and generally increases surface corrosion rates. EVA has been shown to produce acetic acid that catalyzes corrosive processes [2]. According to a previous researchers study, browning of the encapsulant near the center of the cell was the most widely observed failure type at 89.1%, encapsulant browning can have an effect on the power output [10].

Table 1. The History of Fielded EVA Encapsulated PV Modules

Location	Module Mfg.	EVA Grade	Color	Est. Max. Temp. (1)	Time of Observed Color	Construction
Davis, CA	I	A9918	clear	-	3 yrs.	Bifacial
SWRES Las Cruces, NM	II	A9918	brown	-	3-4 yrs.	-
Hawaii	III	A9918P	clear	-	4 yrs.	Glass//Tedlar Laminate
Detroit	III	A9918P	clear	-	4 yrs.	Glass//Tedlar Laminate
California	III	A9918P	clear	-	4 yrs.	Glass//Tedlar Laminate
San Ramon, CA	II	-	light amber	64°C (2)	-	Glass//Al Foil Laminate
San Ramon, CA	III	A9918P	faint yellow	64°C (2)	4-5 yrs.	Glass//Tedlar Laminate
San Ramon, CA	IV	other	light amber	64°C (2)	4-5 yrs.	Glass//Tedlar Laminate
San Ramon, CA	V	A9918	light amber	64°C (2)	-	Glass//Tedlar Laminate
Davis, CA	IV	other	clear	-	4.5 yrs.	Glass//Tedlar Laminate
China Lake, CA	II	A9918	discolored	-	5 yrs.	Glass//Al Foil Laminate?
China Lake, CA	VI	A9918	brown	-	5 yrs.	-
Sells, AZ	IV	other	80% brown	-	6-8 yrs.	Glass//Tedlar Laminate
City of Austin, TX	IV	other	slight brown	60-71°C (2),(3)	7 yrs.	Glass//Tedlar Laminate
SMUD, CA	V	A9918	light amber	65°C (4)	7 yrs.	Glass//Tedlar Laminate
Caples Lake, CA	IV	other	clear	52°C (5)	>7 yrs.	Glass//Tedlar Laminate
Carrisa Plains, CA	IV	other	slight brown	-	8 yrs.	Glass//Tedlar Laminate & Bifacial
John Long, Phoenix, AZ	IV	other	moderate	77°C (2)	8 yrs.	Glass//Tedlar Laminate
Sandia, Albuquerque, NM	V	A9918	light amber	-	8 yrs.	Glass//Tedlar Laminate
SMUD, CA	IV	other	slight brown	77°C (2)	9 yrs.	Glass//Tedlar Laminate
San Ramon, CA	V	A9918P	clear	-	9-10 yrs.	Glass//Tedlar Laminate
Carrisa Plains, CA	IV	other	dark brown	80-90°C (6)	10 yrs.	Glass//Tedlar Laminate & Bifacial
Costa Rica	VII	A9918	clear	-	10 yrs.	Glass//Tedlar Laminate & Tefzel//Tedlar Laminate
Mojave Desert	VI	A9918	clear	-	10 yrs.	Glass//Tedlar Laminate
"Around the World"	VI	A9918	clear	-	10 yrs.	Glass//Tedlar Laminate
Cape Canaveral, FL	II	A9918	discolored	-	10 yrs.	Glass//Al Foil Laminate
SWERS Las Cruces, NM	V	A9918	light amber	75°C (5)	10 yrs.	Glass//Tedlar Laminate

(1) Estimated, no "hard" data available, (summer) measurements taken mostly from back-side of module
(2) Average ambient temperature, plus 30°C
(3) High and low mounted racks
(4) Manufacturer's date
(5) Estimated based on high wind velocity (ambient temperature, plus 20°C)
(6) Modules operated at approximately 2 suns (mirror enhanced)

Figure 6 Case histories of EVA encapsulant discoloration in fielded modules [5]

According to previous reports, browning in the South and West are not surprising when considering the actual solar insolation distribution. Based on published information, the southern and western regions of the United States have greater solar irradiance than the eastern or central regions. [5].

It was also verified based on these findings that due to the approximate nature of the module operation temperature data provided by the module manufacturers, the National Weather Service average maximum temperature data was later used to more accurately correlate the module operation temperatures with EVA discoloration. Based on National

Weather Service Station maximum average daily temperature data modules in Phoenix, AZ potentially operated at annual maximum temperatures greater than other test site locations surveyed. [5].Conclusions taken from the above report indicate that solar insolation in combination with module operating temperature appear to be primary factors in EVA encapsulant discoloration. All reported cases appeared in the South and West where both are comparatively high. This allowed for a better grasp of encapsulant discoloration and the conditions in which it occurs.

2.7 Effect of Series Resistance

Series resistance in a solar cell has three causes: firstly, the movement of current through the emitter and base of the solar cell; secondly, the contact resistance between the metal contact and the silicon; and thirdly, the resistance of the top and rear metal contacts. The main impact of series resistance is to reduce the fill factor (FF), although excessively high values may also reduce the short-circuit current. Series resistance does not affect the solar cell at open-circuit voltage since the overall current flow through the solar cell, and therefore through the series resistance, is zero. However, near the open-circuit voltage level, the IV curve is strongly affected by the series resistance. A straight-forward method of estimating the series resistance from a solar cell is to find the slope of the IV curve at the open-circuit voltage point [7].

Significant power losses are caused by the presence of shunt resistance Rsh). Low Rsh values are caused typically by manufacturing defects, rather than poor solar cell design. Low shunt resistance causes power losses in solar cells by providing an alternate current path for the light-generated current. Such a diversion reduces the amount of current flowing through the solar cell junction and reduces the solar cell’s voltage.

The effect of shunt resistance is particularly severe at low light levels, since there will be less light-generated current. The loss of this current to the shunt therefore has a larger impact. In addition, at lower voltages, where the effective resistance of the solar cell is high, the impact of a resistance in parallel is large [7].

2.8 Bypass Diode Failure:

When one solar cell of the panel is shaded while the others are illuminated, a hot spot could appear and lead to the shaded cell destruction. The bypass diode is an efficient solution to eliminate the “hot spot” and maintain the current delivery [6]. Failed bypass diodes can lead to safety issues.

2.9 Degradation Rates

Arizona state university Photovoltaic Reliability Laboratory researched on 1900 modules in hot-dry climate of Tempe, Arizona and found that the degradation rates lie between 0.6%/year and 2.5%/year depending on the model and manufacturer [3]. The major contributors for power degradation of the modules with glass/polymer modules appeared to be fill factor loss and short circuit loss. National Renewable Energy Laboratories (NREL) reported that the module degradation rate can be as high as 4%/year, but the median and average degradation rates are between 0.5%/year and 0.8%/year [8].

CHAPTER 3

METHODOLOGY

3.1 System description and site layout

The plant is located in Mesa, Arizona. The plant consists of 3,024 modules arranged in 12 rows, 12 strings in each row as can be seen in Figure 1. These modules are mounted on a horizontally fixed tilt (slightly tilted to East), tracking system. The 2 sites that were evaluated as part of this study have two separate SMA 125 KW inverters, disconnect switches and combiner boxes. The plant (composed of two systems, designated as Site 4A and Site 4B; aged 16 years) was initially (first 7 years) installed on a 1-axis tracker (Gilbert, Arizona) and then moved to another site (Mesa, Arizona) where the modules were reinstalled at a fixed horizontal tilt (9 years).

Table 1 System Location

System	Location	Latitude	Longitude	Elevation	Year Commissioned
Site 4A & 4B	Mesa, AZ	33.4° N	111.7 W	1241ft	1997

Table 2 System Description

System	Tilt/ Orientation	DC Rating (kW)	AC Rating (kW)	Years fielded	Module Type	No. of Modules	Inverter
Site 4A	Horizontal fixed tilt.	113.4	100	16	BRO 1	1512	SMA 125 kW
Site 4B		113.4	100	16	BRO 2	1512	SMA 125 kW

As shown in figure 6 each system consists of 6 rows with 12 strings in each row oriented in the north-south direction. Each string has 21 modules connected in series as shown in Figure 9. The modules are installed with horizontal tilt.

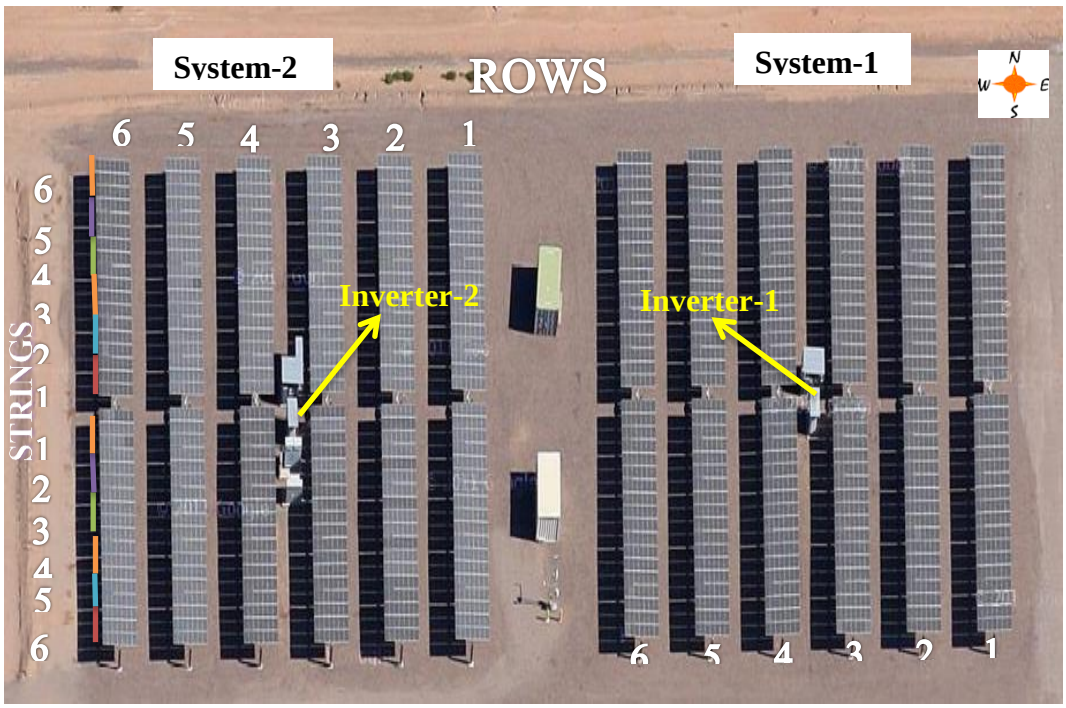

Figure 8 Site 4A & 4B Layout

Table 3 Module and String nameplate rating

Model	Design		Nameplate rating				
		Isc (A)	Voc (V)	Imax (A)	Vmax (V)	Pmax (W)	FF (%)
Module BRO 1 , BRO 2	Frameless Glass/Polymer	**4.8**	**21.7**	**4.4**	**17**	**71.8**	**75**
BRO 1, BRO 2 String	21 modules/ string	**4.8**	**455.7**	**4.4**	**357**	**71.8**	**1575**

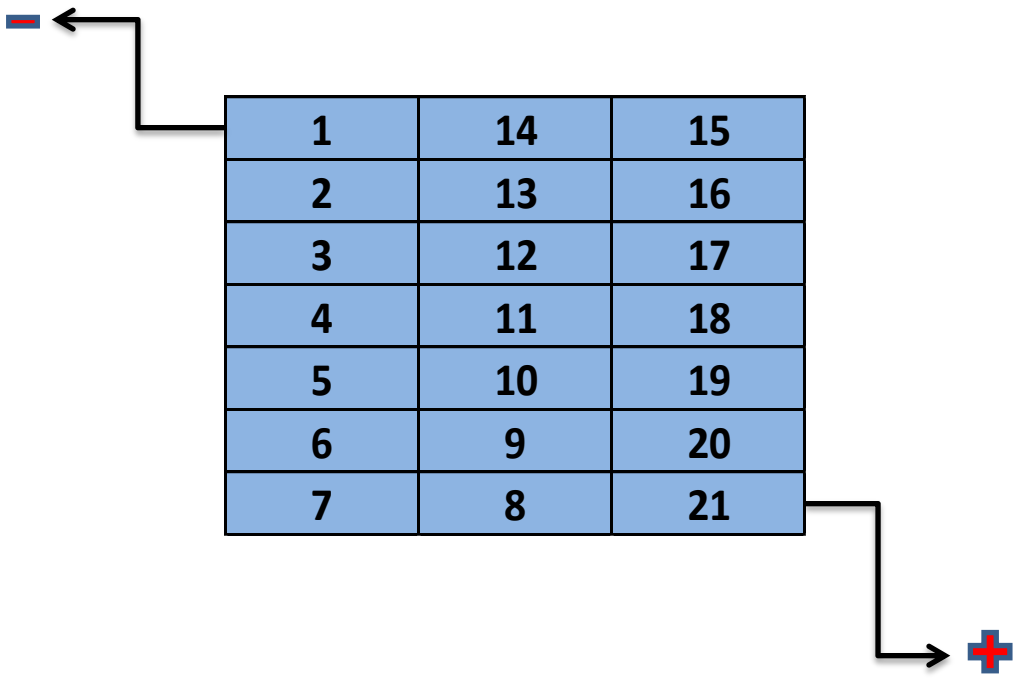

Figure 9 Site-4A&4B string circuit diagram

String circuit connection at site 4A and 4B. The numbers indicate the modules and their position

3.2 Data Collection and Processing:

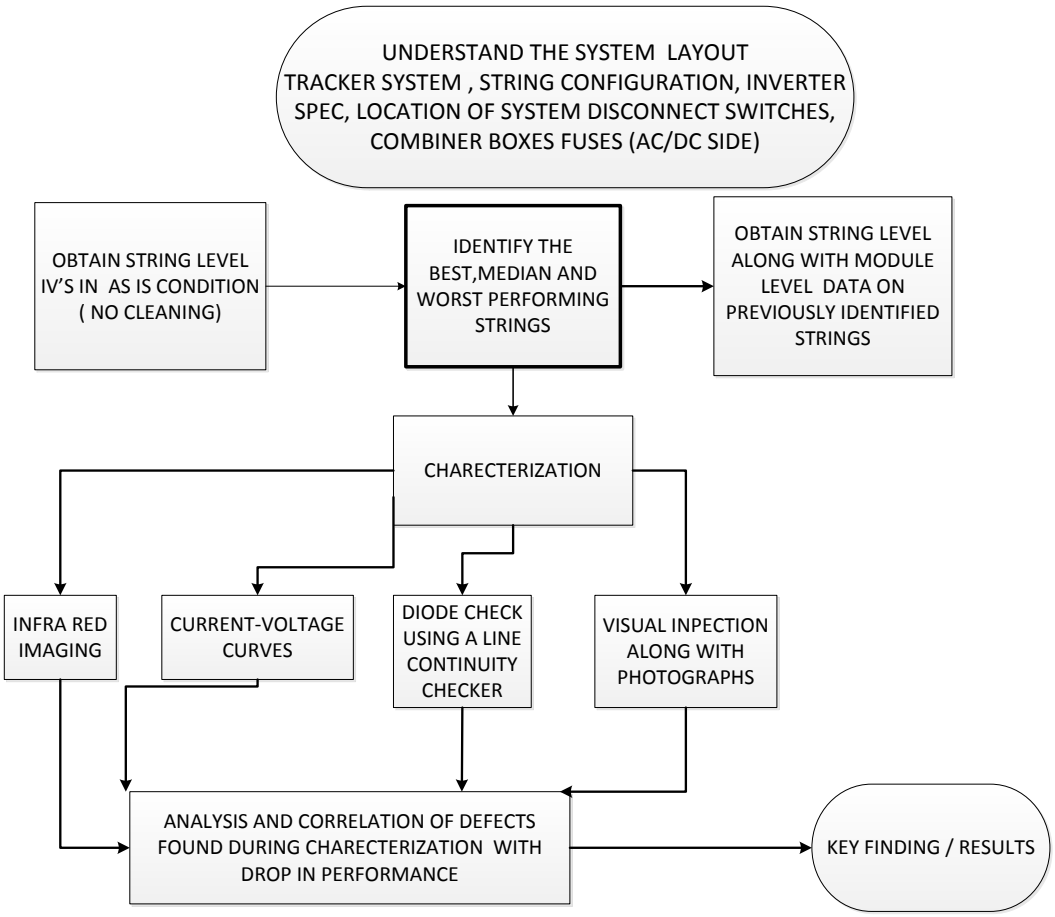

Figure 10 Flowchart of Tasks carried out.

3.2.1 Equipment Used On Site:

a. Daystar's DS-100C I-V curve tracer

b. Laptop computer with IVPC 3.0 software (for curve tracer)

c. Fluke temperature sensor with T and K-type thermocouples

d. Inclinometer.

e. Diode checker

f. 1-monocrystalline and 1- polycrystalline reference cell.

g. Curve tracer cables.

h. Fluke TI-55 Infra-Red imaging camera.

i. Safety equipment.

j. Fluke digital Multimeters.

k. Module cleaning equipment

l. Ice Packs (for field baseline testing)

m. Insulation boards for causing a shading effect to check for failed diodes.

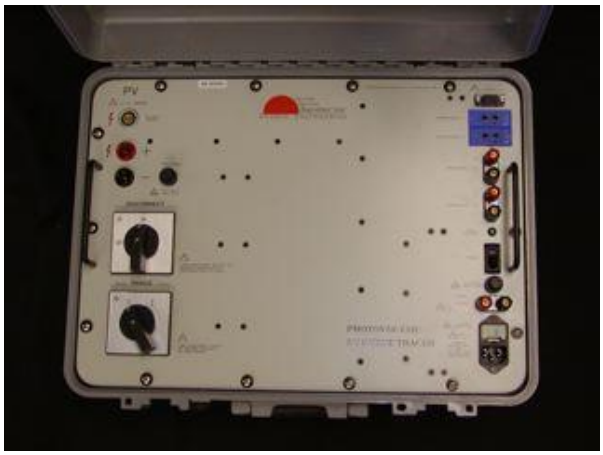

Figure 11 Daystar I-V curve tracer

3.2.2 On site activities

The first step in the evaluation of the 2 PV systems was initiated by gaining an understanding of the system's layout which included: understanding how the strings were connected; how many modules comprised a string; location of the disconnect switches and combiner boxes. Safety was of the highest priority which is why the strings were isolated from both DC and AC sides and the fuses removed as a precautionary measure.

3.2.3 Naming Convention

The next step was to develop a naming convention which would help identify each string in each row, for both systems. This naming convention was strictly adhered to: A sample naming convention which is illustrated below, where (from left-right) S/N stands for south or north respectively because the modules were mounted across the north-south direction. Also, 1/2 stands for system-1 or system-2, 4/3 stands for row number and 2/1 stands for the string number. The same modules were used in both system-1 and 2. The modules from Site 4A are referred to as BRO 1 and modules from Site 4B, BRO 2.

S-1-4-2 **N-2-3-1**

DIRECTION-SYSTEM #-ROW #-STRING #

Figure 12 Naming convention

3.2.4 I-V measurements of modules and strings

The current-voltage (I-V) curve provides module and string performance parameters such as such as maximum power (Pmax), short circuit current (sc), open circuit voltage (Voc), and fill factor (FF), as shown in the screenshot below in Figure 13.The I-V's were taken by first switching off the ac/dc disconnect switches followed by removing the fuses at the combiner box. It was always ensured that the measurements were taken under clear and sunny skies at an irradiance level above 800 w/m^2. I-V curves played a very important role in the entire study because they helped determine the high, median and low performing modules and strings, losses due to soiling, degradation data, diode failures, and module series resistance.

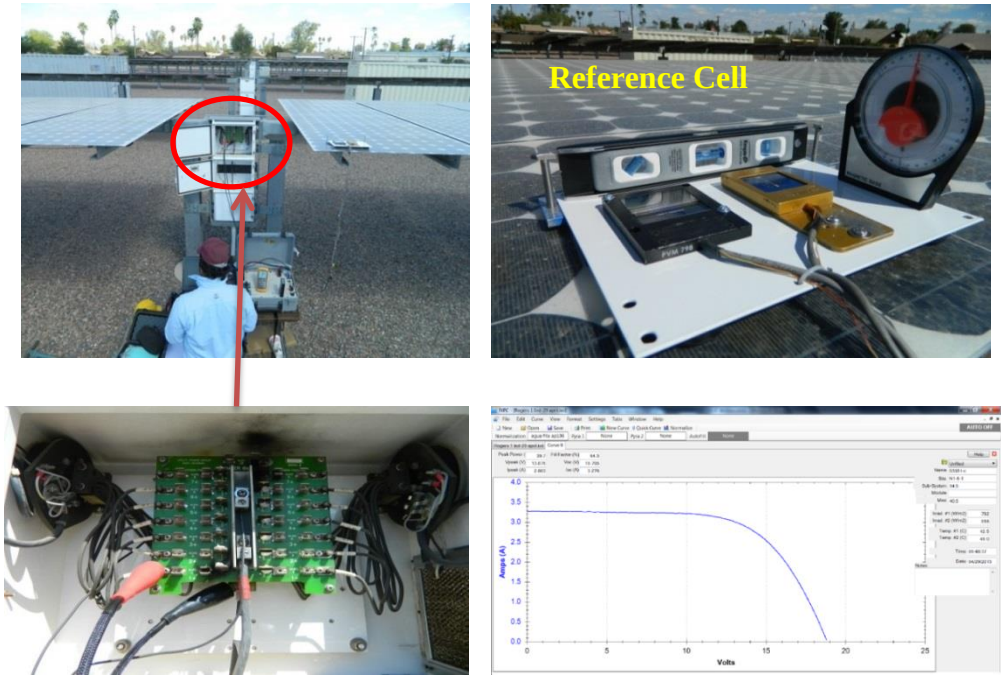

Figure 13 I-V setup & I-V generated through software

3.2.5 Baseline I-V measurements for modules

Baseline tests had to be completed to obtain the voltage and current temperature coefficients, voltage (β), and current (α) to translate the measured data into standard test conditions (STC). A few select modules in the power plant were cooled using ice cubes and styrofoam boards with reflective surfaces to lower the module's temperature. The temperature was monitored by using thermocouples attached to the back sheet of the module at the center of a cell. Once the temperature fell between 12° to 18° Celsius, the ice cubes were removed and the module surface was dried with dry rags to eliminate moisture. Ten I-V curves were taken between 18°C to 45°C and with irradiance of approximately 1,000 W/m^2.

Figure 14 Module cooled using ice and Styrofoam.

3.2.6 Translation procedure with the ASU-PRL template:

Once the IV curves were obtained on site, the IVPC software would display important parameters of that string/module. These I-V curves were later translated to STC conditions via an automated Microsoft Excel spreadsheet developed by ASU-PRL. The curves were translated using the temperature coefficients obtained from the baseline measurements. This data was used for further analysis.

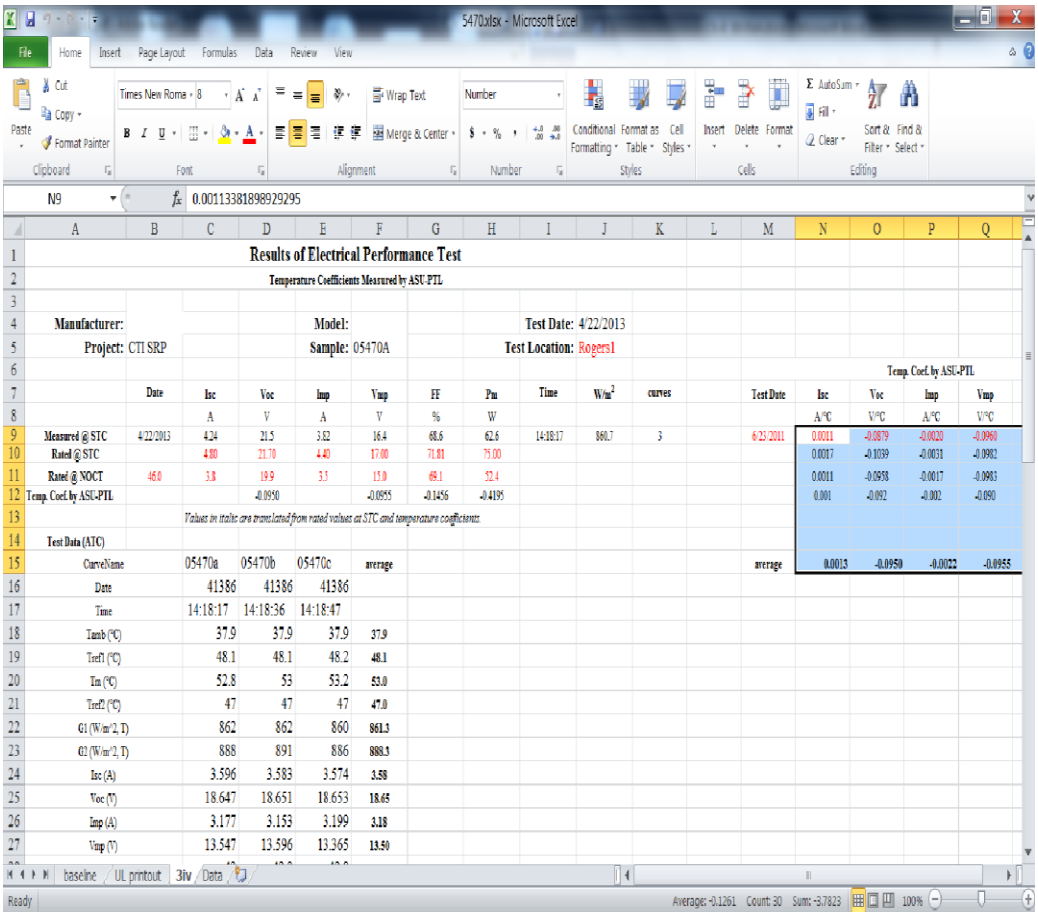

Figure 15 ASU-PTL template for I-V curves translation

3.2.7 I-R imaging for identifying Hotspots

This is a thermal diagnostic test that was conducted using a Fluke TI-55 IR camera. The purpose of this test was to determine the module's ability to withstand localized heating. This localized heating could occur when a cell is in a string of cells connected in series and is negatively biased. In this condition, the cell can dissipate power in the form of heat instead of producing electrical power. This happens when the current produced by a given cell is lower than the string current. Cracked, shaded cells, broken interconnects, mismatched cells and/or failed bypass diodes also can cause hotspots. A drop in performance may be seen due to all the above mentioned reasons. If the cells in the module showed a temperature difference of more than 10-15°C when compared to rest of the cells, they were classified as hot spots. The steel cross beams supporting the modules did not have any effect on heating the modules. However a general observation was made on how all modules had hotter junction boxes.

Figure 16 Fluke TI-55 IR camera

3.2.8 Visual Inspection

Visual inspections are performed to visually verify defects in the module. The defects are recorded on a template sheet along with clear photographs. The template sheets cover all module defects appearing on areas such as the back sheet, frame ground points, metal contacts on the cell, glass, seals etc. The inspection starts from the back sheet to the front end or vice versa. Defects that are found in this stage are crucial as they can be related to causes in drops of performance. These defects could be caused by prolonged exposure to extreme conditions, improper installation and handling, or manufacturer's defects. Each module was inspected for defects such as encapsulant browning, encapsulant delamination, broken glass; interconnect breakages etc, using ASU-PRL's check list of visual defects shown in Figure 17.

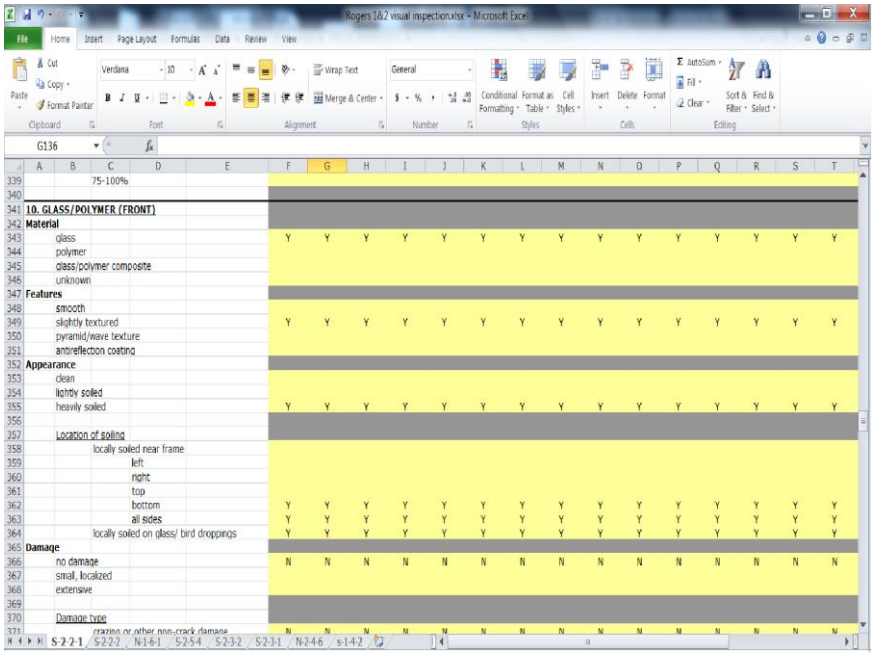

Figure 17 ASU-PRL visual inspection checklist

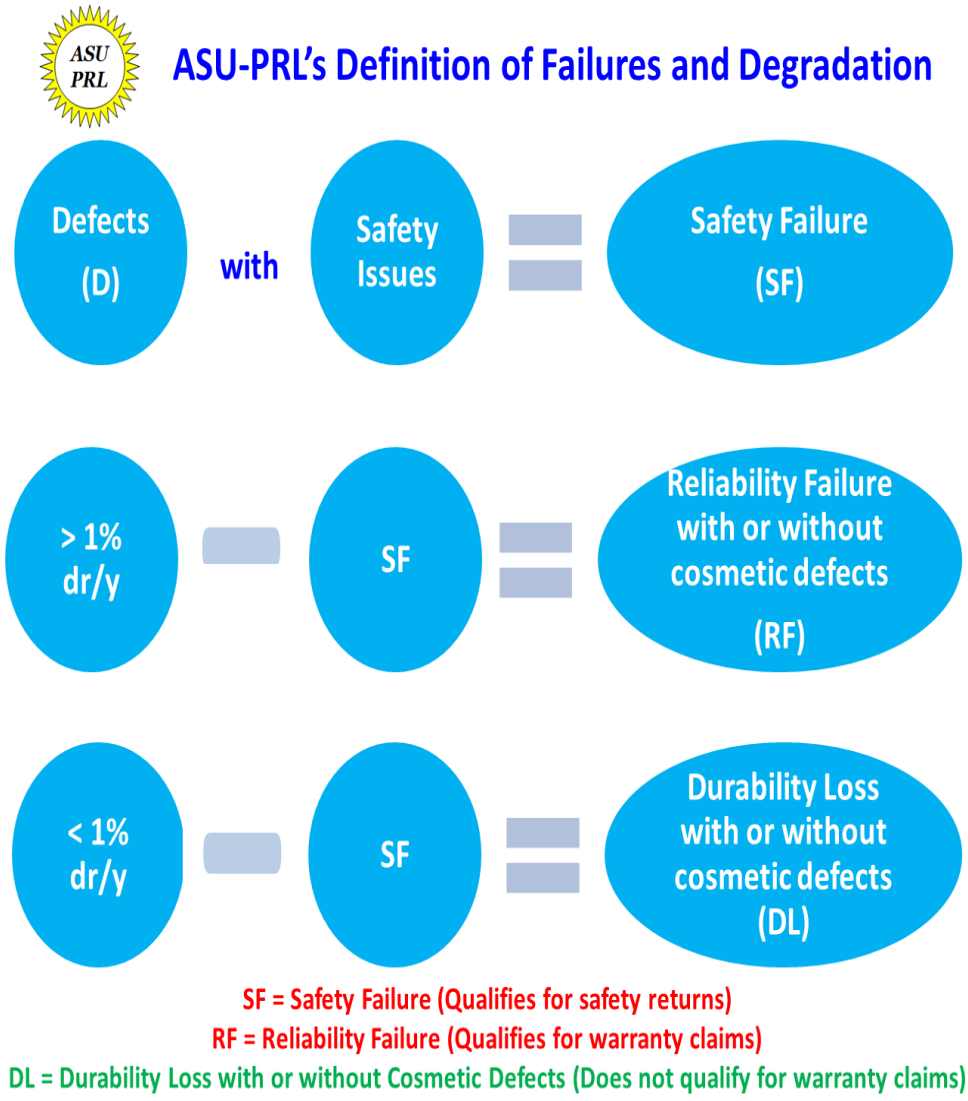

Figure 18 Classification of Defects into Failures and Reliability Issues

3.2.9 Diode and line continuity check

A diode checker was used to check for failed bypass diodes. This equipment consists of a transmitter and a receiver. The transmitter was connected to the common positive and negative terminals at the combiner box. The internal layout of the combiner box provided easy connection points since 12- strings could be checked at once by connecting the transmitter at one combiner box. The receiver was then held perpendicular to the bus bars; this can be done either through the front glass surface or the back sheet of the module. The receiver beeps and blinks a series of lights to show there is continuity in the bus bars and the string interconnects. The number of led lights blinking signified the strength of the signal. A flow chart illustrated below shows how the beeping noise and no beeping noise relates to the circuit continuity or occurrence of failed bypass diodes.

Figure 19 Transmitter and Receiver; diode checker

The test began when the modules were not shaded and the receiver was placed on bus bars of each string associated with diode. If no beeps were heard from the receiver, there were two possibilities to consider. 1) Either the module has broken interconnects or 2) its bypass diode has failed in the short circuit mode. Broken interconnects can be visually verified if the receiver does not beep over the busbar. If no broken interconnects are observed then a bypass diode failure can be suspected. This can be cross verified with the corresponding modules I-V curve or I-R image of the diode. If the receiver beeped on all bus bars, then half of the string was shaded and the receiver was placed on the bus bars of the shaded string underneath the module. If the receiver beeps in that case, it indicates that the diode is functional. If the receiver does not blink, then the diode has failed in open circuit condition. Only 2 failed bypass diodes (one in each system) were recorded at the Site 4A and 4B.

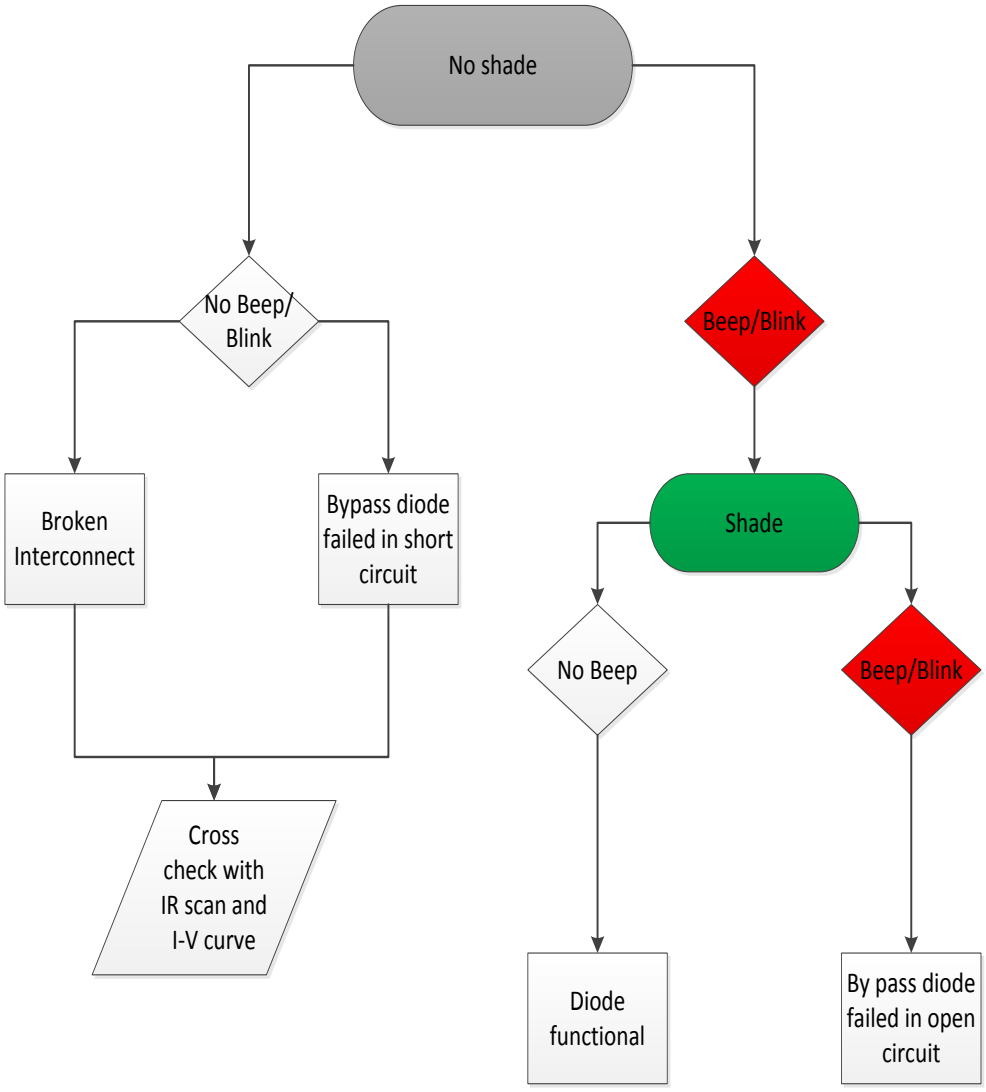

Figure 20 Flowchart for detection of failed diodes and broken interconnects using diode checker

3.2.10 PID in Hot- dry climatic conditions

The modules from the best, median, and worst strings were arranged based on their position in the string and the overall percentage power degradation of each module in the string was plotted in a scatter plot. A trend line was drawn for each of the plots to reveal a constant trend in the degradation of modules with respect to their position (proximity to ground) in the string.

String connection at systems -1 and -2 were analyzed and due to the absence gradual degradation based on the position of the modules along the trend line, it was concluded that there was no PID.

3.2.11 Series resistance (Rs)

The series resistance of modules was calculated by first normalizing the measured I-V curve to STC, after which the slope of the last ten data points (close to Voc) was calculated to obtain the Rs value.

3.3 Data Analysis

The best, median, and worst strings based on power were selected. From these selected strings the best, median, and worst modules were then selected. The degradation %/year for Isc, Imax, Voc, Vmax, FF and Pmax were calculated. The parameters for these selected strings and modules were analyzed using the box plot feature in Minitab. The primary parameter responsible for the cause of power degradation is identified from the graph by choosing the median of the 5 parameters falling close to the median of the P_{max} degradation (%/year). This is correlated with the defects seen in the visual inspection in order to identify the failure mode.

CHAPTER 4

RESULTS AND DISCUSSION

This chapter explains how various I-V parameters of the evaluated modules affected their degradation in Pmax. The modules from the best, median, and worst strings were separated into best, median, and worst modules. These modules were analyzed for durability and reliability issues. A detailed explanation of their degradation analysis, visual inspection results, potential induced degradation, along with soiling losses and wind effect analysis are also discussed in this chapter.

4.1 Site 4A Performance Degradation Analysis

The performance degradation calculations for these two systems were done by using the manufacturer's nameplate rating. The nameplate data was compared to the data of an independent source's data base for confirmation and it was later realized that the manufacturer's nameplate rating was overrated by approximately 5%. Since earlier studies utilized manufacturer's nameplate information, for the sake of consistency it was decided that this study should also use the manufacturer's nameplate rating.

As explained in an earlier chapter the best, median, and the worst strings were analyzed extensively to diagnose the durability issues. Usually the worst performing modules will bring out the reliability issues and the best performing modules will bring out the durability issues.

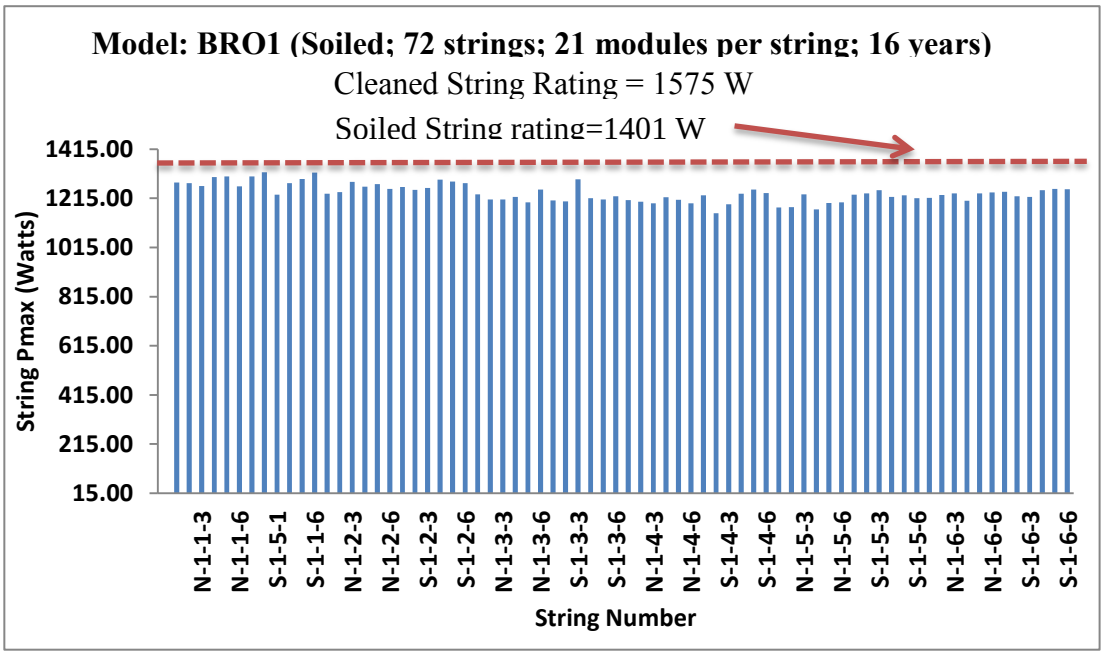

Figure 21 Strings Pmax for model BRO-1 in site -4A

.

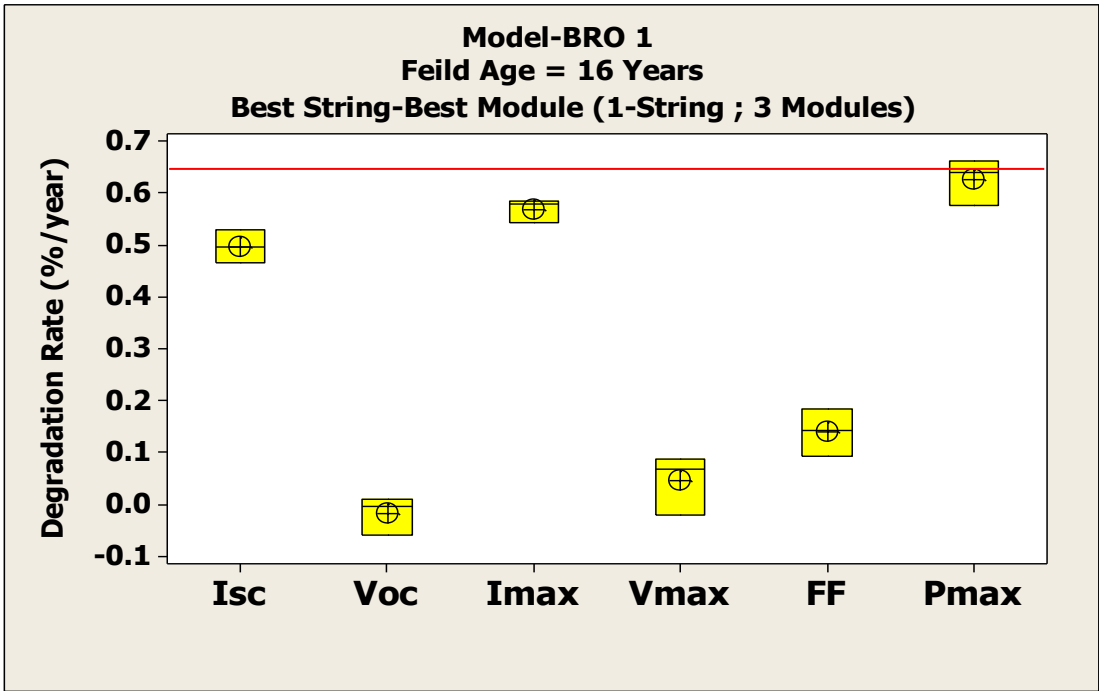

Figure 22 Plot for various I-V parameters degradation (%/Year) for the best string-best modules

The plots from Figure 22 and Figure 24 show that Imax and Isc have contributed to the overall degradation in Pmax. The median of the Pmax degradation rate is close to the median of Imax and Isc. This is due to significant levels of encapsulant browning which causes optical losses. A slight increase in series resistance is indicated by a drop in Vmax.The histogram in Figure 23 shows a normal distribution for the series resistance values (Rs) for the 30 best modules in Site 4A and 2. These modules experienced drop in power mainly due to optical losses, their low series resistance did not play a substantial role.

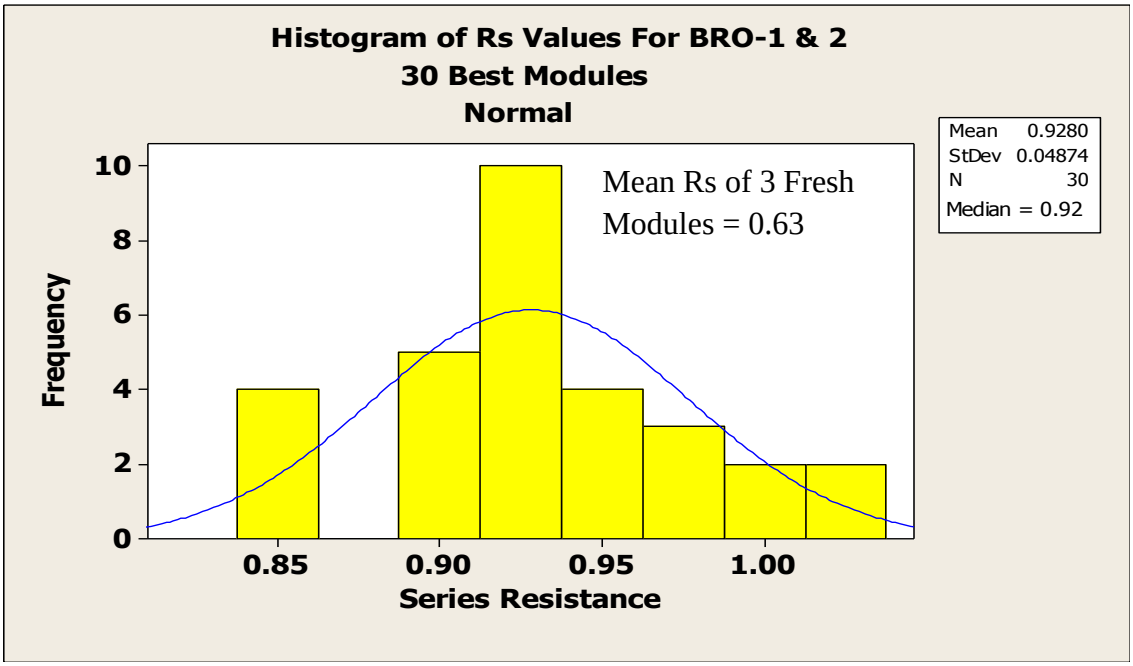

Figure 23 Histogram on Rs values for 30 best modules

Table 4 Series Resistance comparison with fresh modules.

	Fresh Modules	Best 30 Modules
Mean Rs	0.63	0.93
Median Rs	0.63	0.93
% increase	N/A	30.30%

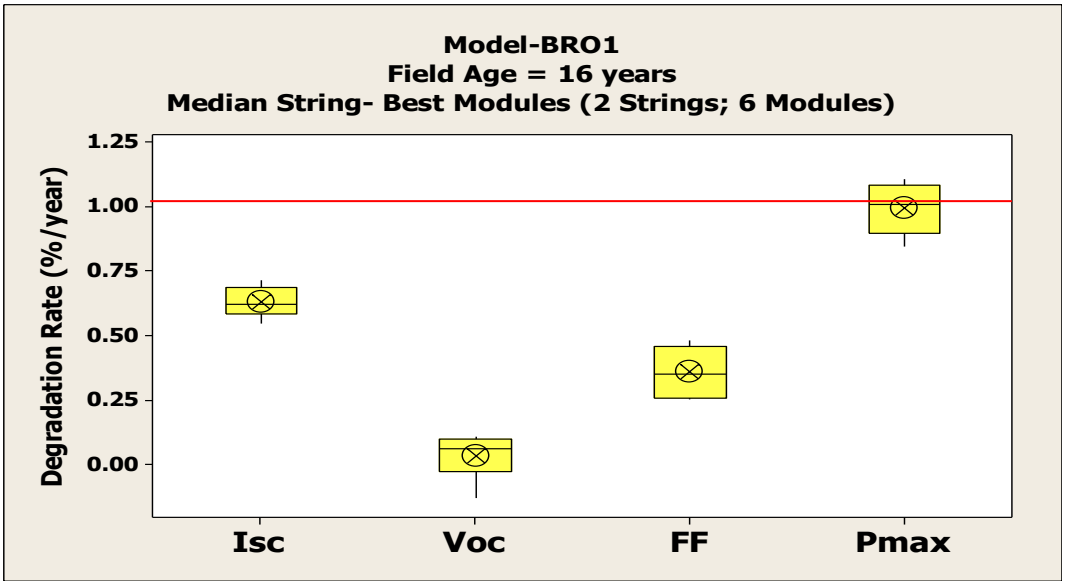

Figure 24 Plot for various I-V parameters degradation (%/Year) for the Median string- best modules.

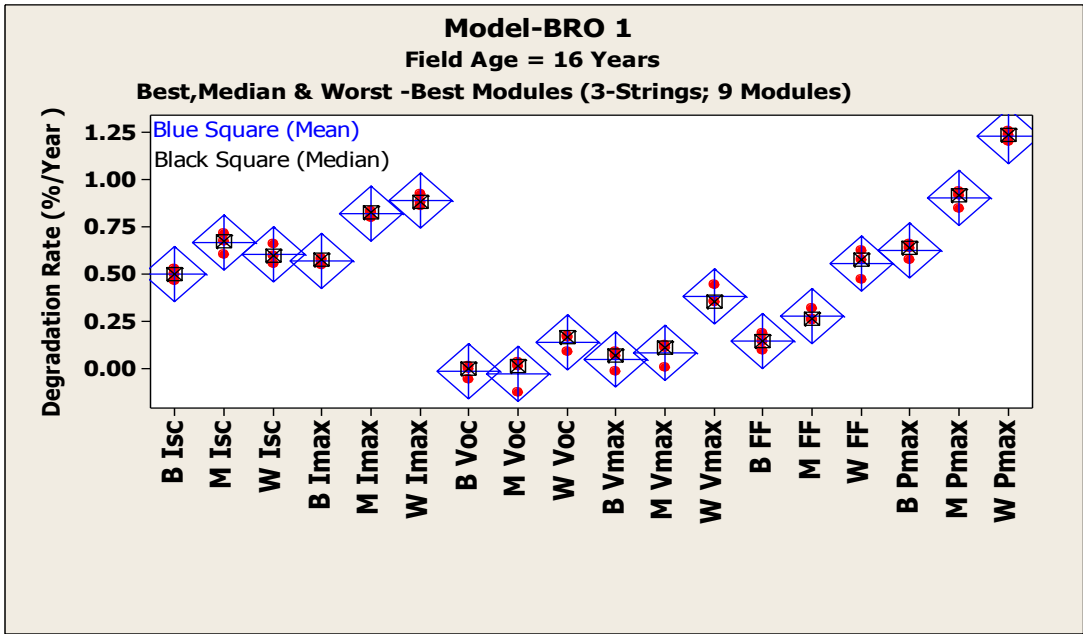

Figure 25 Summary plots for various I-V parameter degradation (%/year) for best modules in Best, Median and worst strings in Site 4A.

The plot in figure 25 shows a summary of the best modules performance degradation rate for various parameters in the best, median, and worst strings. It can be seen once again that the Imax and Isc and are observed to be the major contributors for Pmax degradation in these strings due to a combined effect of encapsulant browning and an increase of more than 30 % in series resistance shown by the degradation in Vmax

A steep drop in Imax and Isc are the parameters responsible for the degradation of Pmax, due to encapsulant browning. Drop in Vmax and FF is attributed to the series resistance increase.

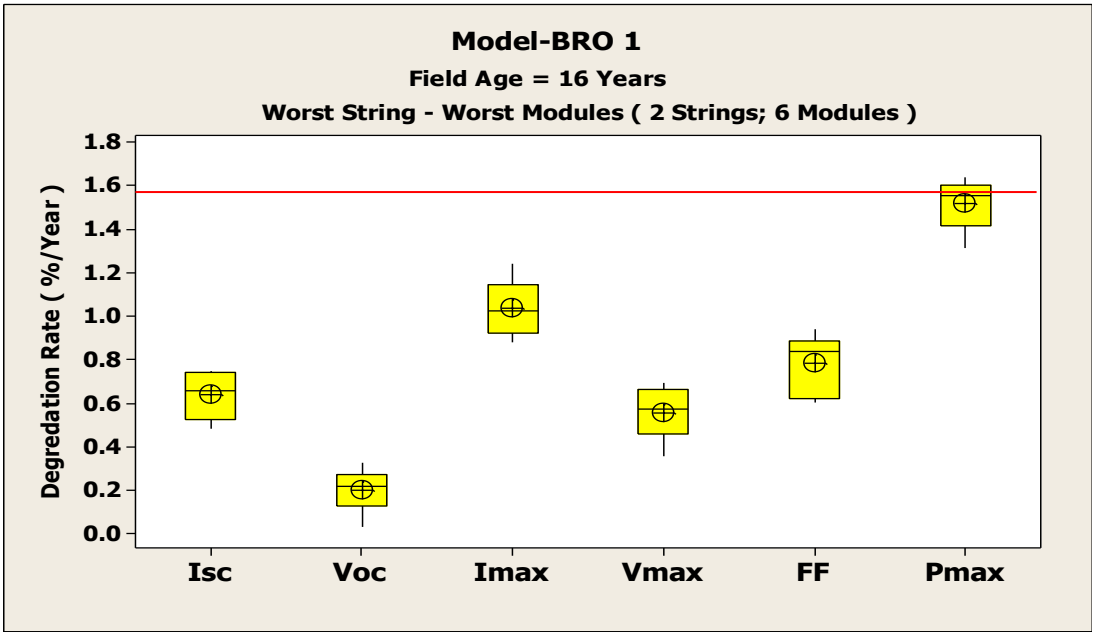

Figure 26 Plot for various I-V parameter degradation (%/year) for worst string-worst modules.

Imax, Isc are the major contributors for Pmax degradation, this is because these modules have encapsulant browning indicated by a higher drop in Imax and Isc.

B = **B**est string; M = **M**edian string; W = **W**orst string

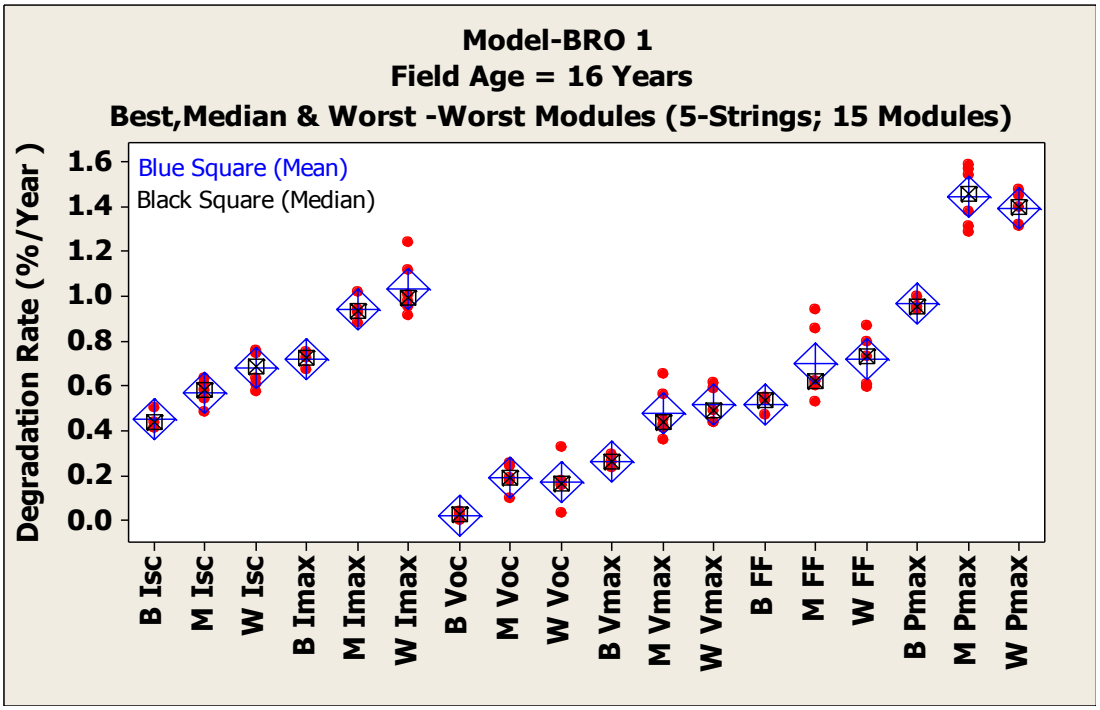

Figure 27 Summary plots for various I-V parameter degradation (%/year) for worst modules in Best, Median and worst strings.

The plot in figure 27 shows a summary of the worst performing modules degradation rate from the best, median, and the worst strings. A drop in Imax and Isc along with FF and Vmax signifies encapsulant browning coupled with high series resistance.

Table 5 I-V Parameter order of Influence on Pmax degradation

	Best Modules	Median Modules	Worst Modules
2 BEST STRINGS	**Imax> Isc>FF>Vmax (Low Series resistance and high transmittance Losses due to encapsulant browning)**	**Imax>Isc>FF>>Vmax**	**Imax>Isc>FF>>Vmax**
2 MEDIAN STRINGS	**Imax>Isc>FF>>Vmax**	**Imax>Isc>FF>>Vmax**	**Imax>Isc>FF>>Vmax**
2 WORST STRINGS	**Imax>Isc>FF>>Vmax**	**Imax>Isc>FF>>Vmax**	**Imax> Isc>FF>Vmax (Encapsulant browning high series resistance.**

The table above summarizes results on the analysis of the modules from the best, median and worst strings of Site 4A. It can be seen that the Imax is affected first followed by the Isc and in the best modules in the best string, this is because of the effect of encapsulant browning.The worst modules have high series resistance (due to solder bond fatigue).The median modules in three different strings have the same order of influence of parameters on Pmax degradation.

Table 6 Summary- of degradation and failure Modes and their effects on performance parameters for Model BRO-1.

Module Quality	Primary Parameter Affected	Primary Degradation/Failure Mode
Best Modules	**Imax, Isc**	**Optical losses due to encapsulant browning.**
Worst Modules	**Imax, Isc , FF Vmax>>Voc**	**Encapsulant browning and high series resistance due to solder bond fatigue.**

4.2 Site 4B Performance Degradation Analysis

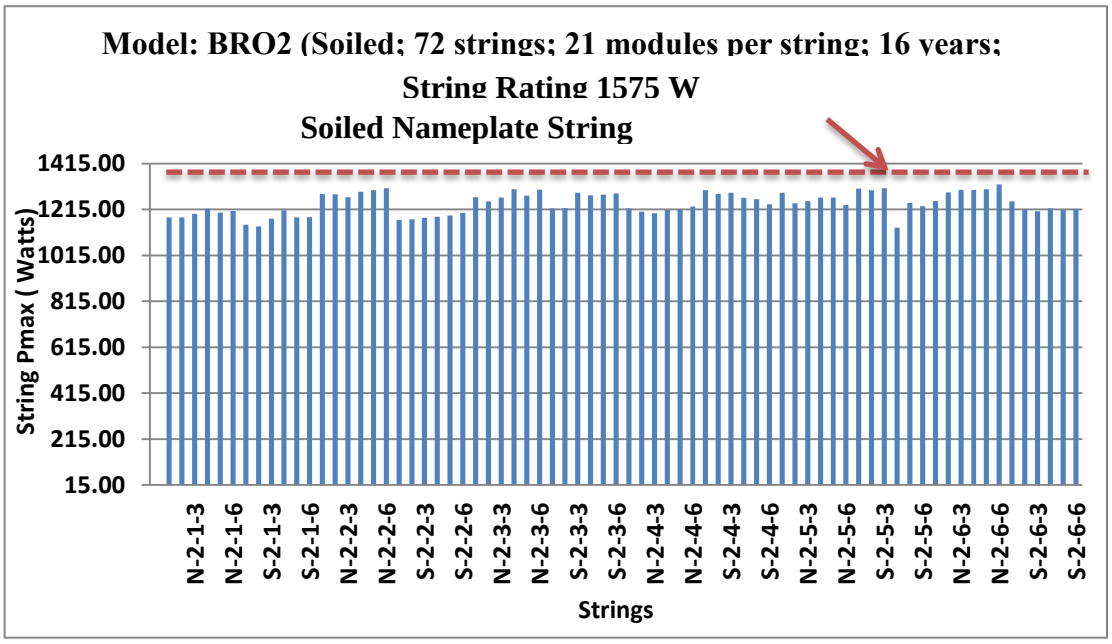

Figure 28 Strings Pmax for BRO 2 modules in site -4B

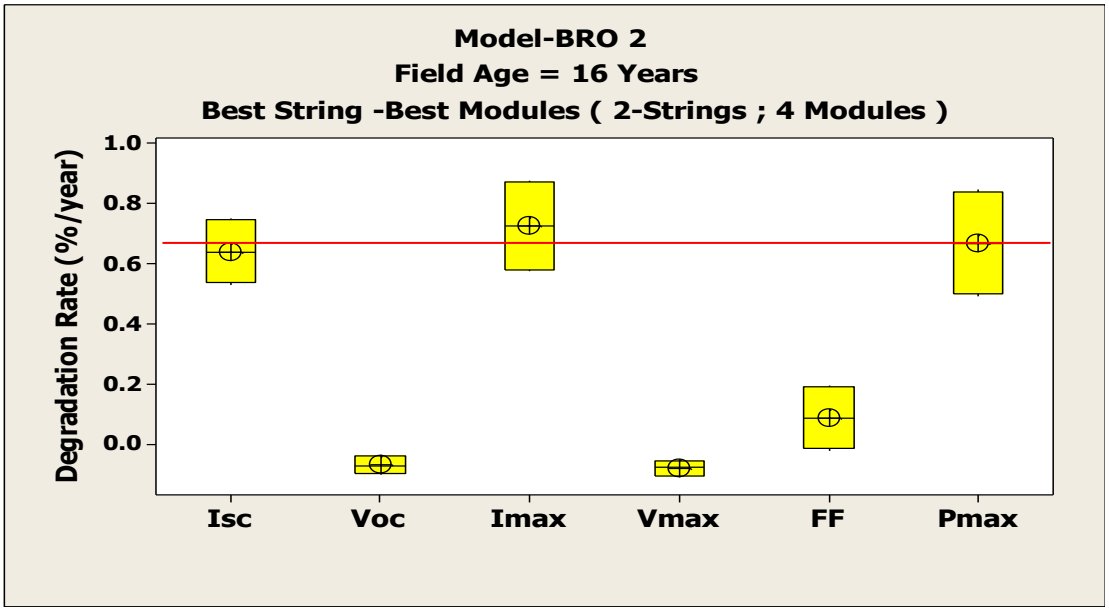

Figure 29 Plot for various I-V parameter degradation (%/year) for best string- best modules.

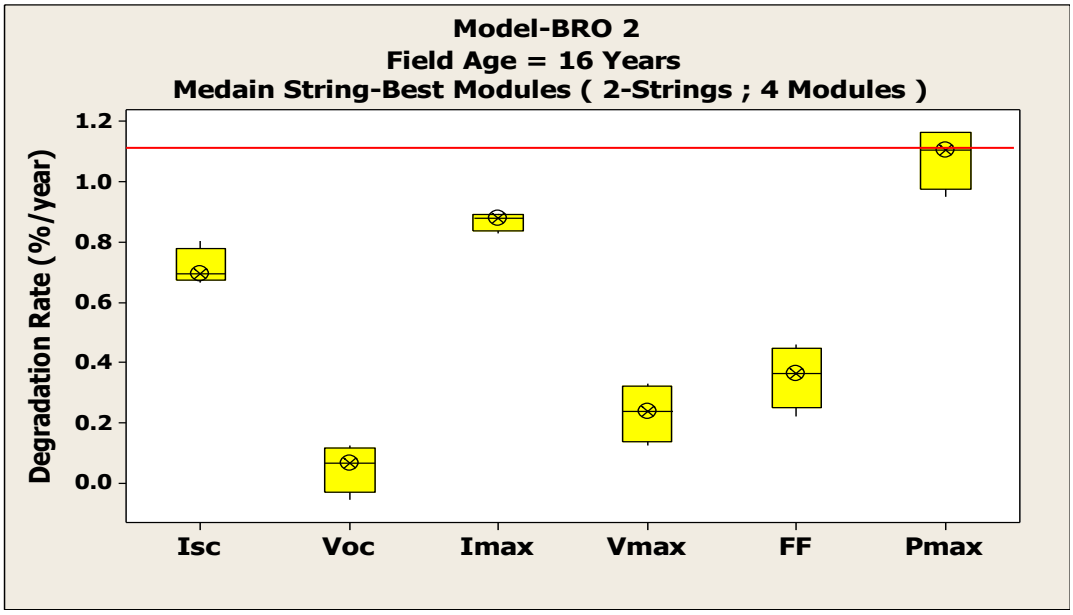

Figure 30 Plot for various I-V para meter degradation (%/year) for median string- best modules

The effect of transmittace issues can be seen due to drop in Imax and Isc in the best and median modules as shown in Figure 29 and Figure 30.

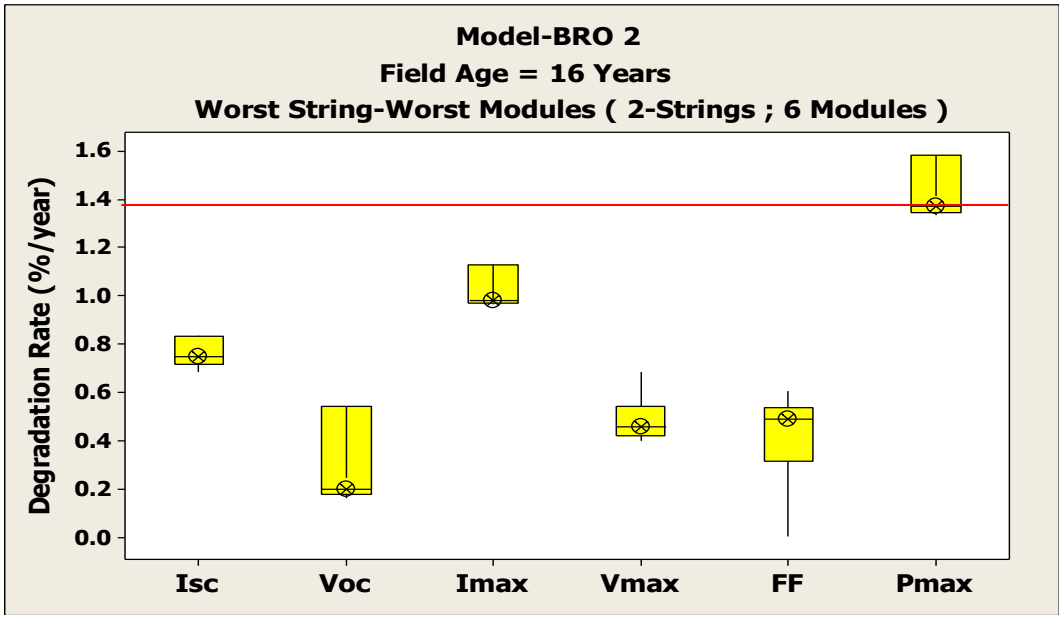

Figure 31 Plot for various I-V parameter degradation (%/year) for worst string- worst modules

The drop in Imax and Isc indicates high levels of encapsulant browning the increase in Imax and FF indicates increased level of series resistance.

	Best Modules	Median Modules	Worst Modules
2 BEST STRINGS	**Imax>Isc>FF (Encapsulant browning and low series resistance values)**	**Imax>Isc>FF>Vmax**	**Imax>Isc>FF>>Vmax**
2 MEDIAN STRINGS	**Imax>Isc>FF>Vmax**	**Imax>Isc>FF>Vmax**	**Imax>Isc>FF>Vmax**
2 WORST STRINGS	**Imax>Isc>FF>Vmax**	**Imax>Isc>FF>Vmax**	**Imax>Isc>FF>Vmax High optical losses and series resistance**

Table 7 I-V Parameter order of Influence on Pmax degradation

The table above summarizes results on the analysis of the modules from the best, median and worst strings of Site 4B. It can be seen that the Pmax is affected by the Imax followed by the Isc and in the best modules in the best string, this is because of the effect of encapsulant browning .The worst modules have high series resistance (due to solder bond fatigue) and optical losses due to browning.The median modules in three different strings have the same order of influence of parameters on Pmax degradation.

Table 8 Summary of degradation and failure Modes and their effects on performance parameters for Model BRO 2.

Module Quality	Primary Parameter Affected	Primary Degradation/Failure Mode
Best Modules	**Imax, Isc**	**Transmittance losses due to high discoloration, low series resistance**
Worst Modules	**Imax, Isc ,FF**	**Transmittance losses along with high series resistance.**

4.3 Degradation rates

The histogram shown in Figure 32 indicates the mean and median degradation rate of modules in Site 4A as 1.078%/year and 1.1%/year respectively. The degradation values used for these plots were computed after considering a soiling loss of 11% based on Figure 52 .The red dotted line indicates the 20/20 warranty line which is inserted at 1%/year; modules /strings on the left of this line will meet warranty requirements whereas modules/strings on the right of the line will not and are entitled for replacement.

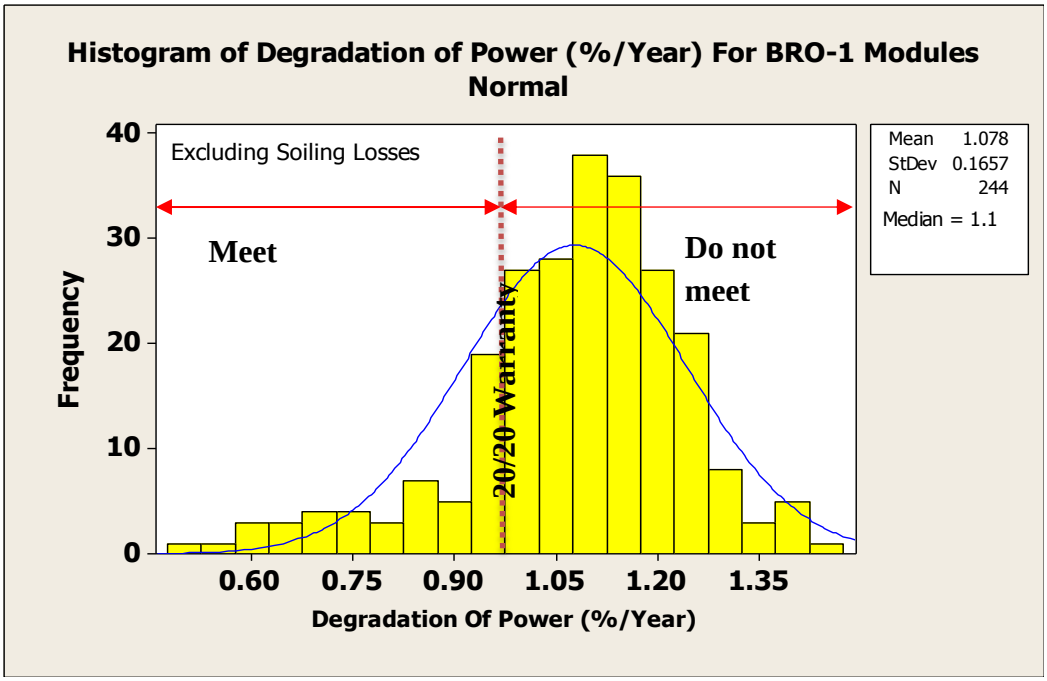

Figure 32 Histogram of Power Degradation (%/year) for all BRO 1 modules

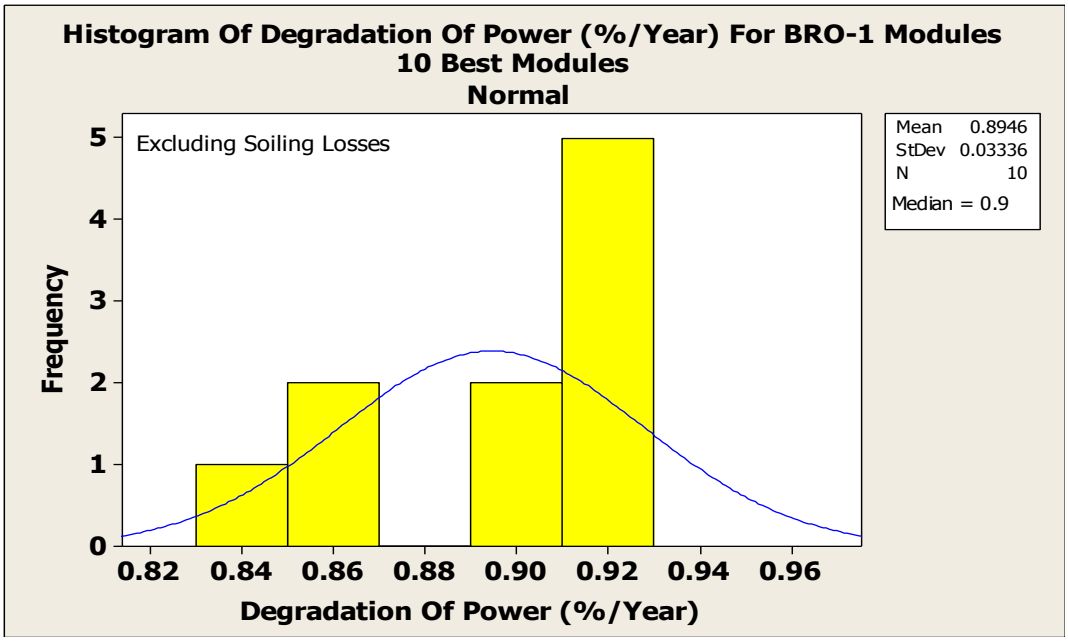

Figure 33 Histogram of Power Degradation (%/year) for 10 Best modules for BRO 1

The histogram shown in Figure 33 indicates a mean and median value of 0.89%/year and 0.9%/year respectively, for the 10 best modules selected from the best string. This indicates that all the best modules are still producing enough power to meet the warranty requirements. This module's Pmax is primarily affected by encapsulant browning and very low series resistance; same is the case for the 10 best modules in Site 4B.

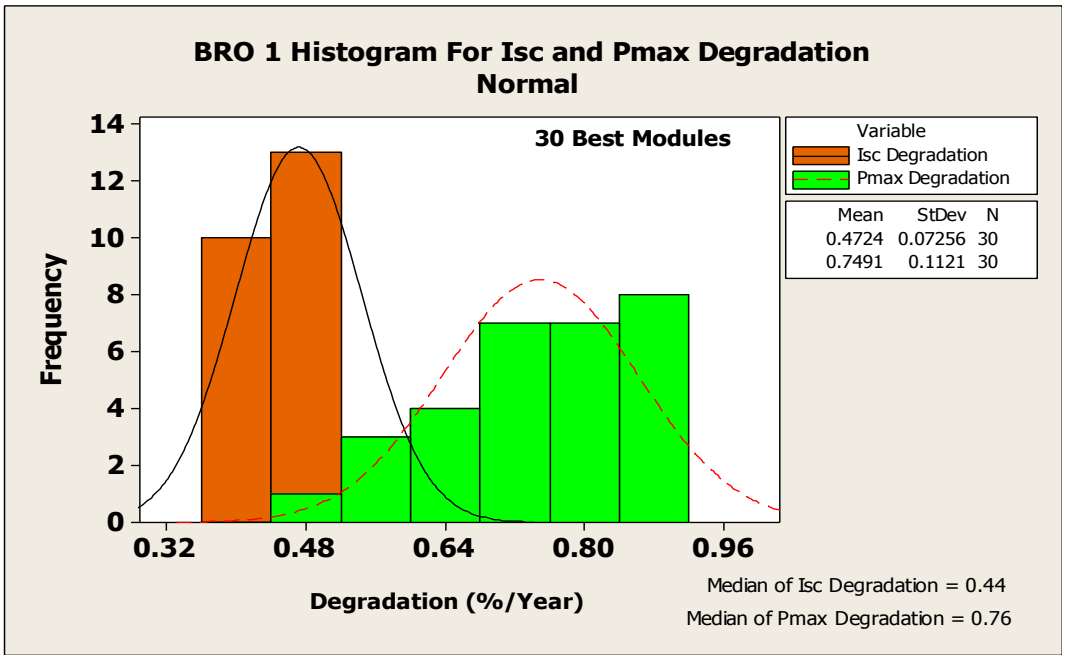

Figure 34 Histogram on Isc and Pmax degradation for 30 best modules in BRO 1

Since, Pmax, FF, Voc and Isc are related through the equation Pmax= Voc*FF*Isc, drop in any one of these parameters can cause a drop in power. Therefore, in the case of the best modules the encapsulant browning causes an optical loss which affects the Isc causing a drop in power. If the Voc drop is considered zero, and the drop in Isc is equal to the drop in Imax 60% of the contribution to the drop is seen due to encapsulant browning and the remaining percentage can be calculated to obtain the contribution made by increase in series resistance.

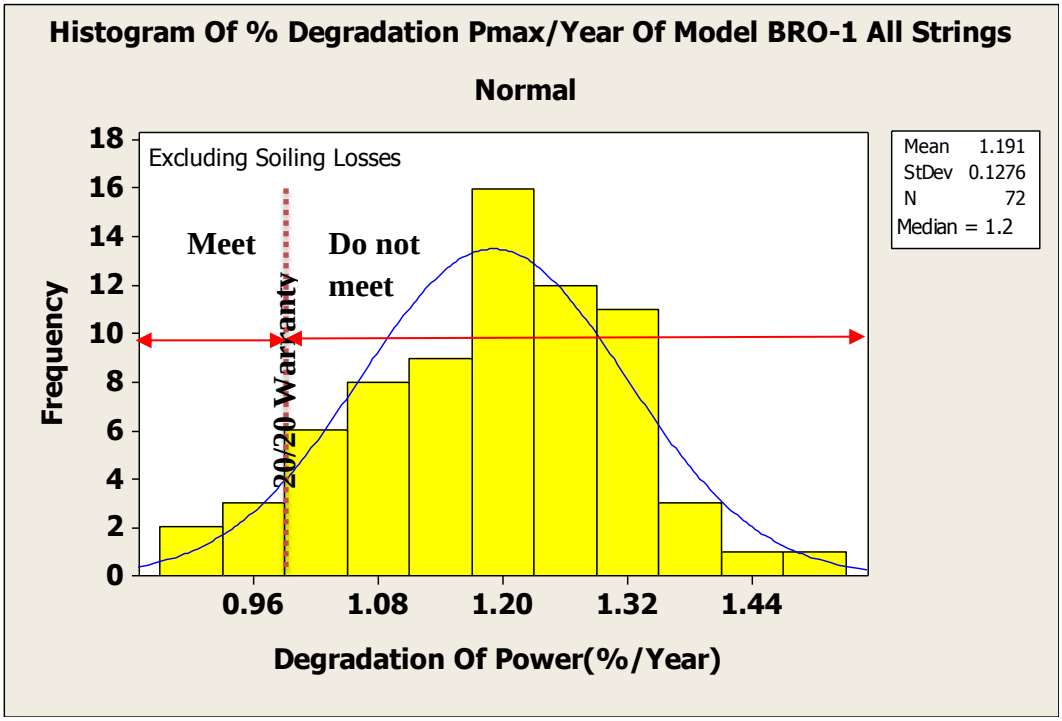

Figure 35 Histogram of Power Degradation (%/year) for all strings with BRO 1 modules.

The histogram in Figure 35 shows a mean degradation rate of 1.19%/year and a median degradation rate of 1.2%/year. A slightly higher degradation rate of strings as compared to the modules may be attributed to soiling losses, intermodule cable losses, and mismatch of modules within the string.

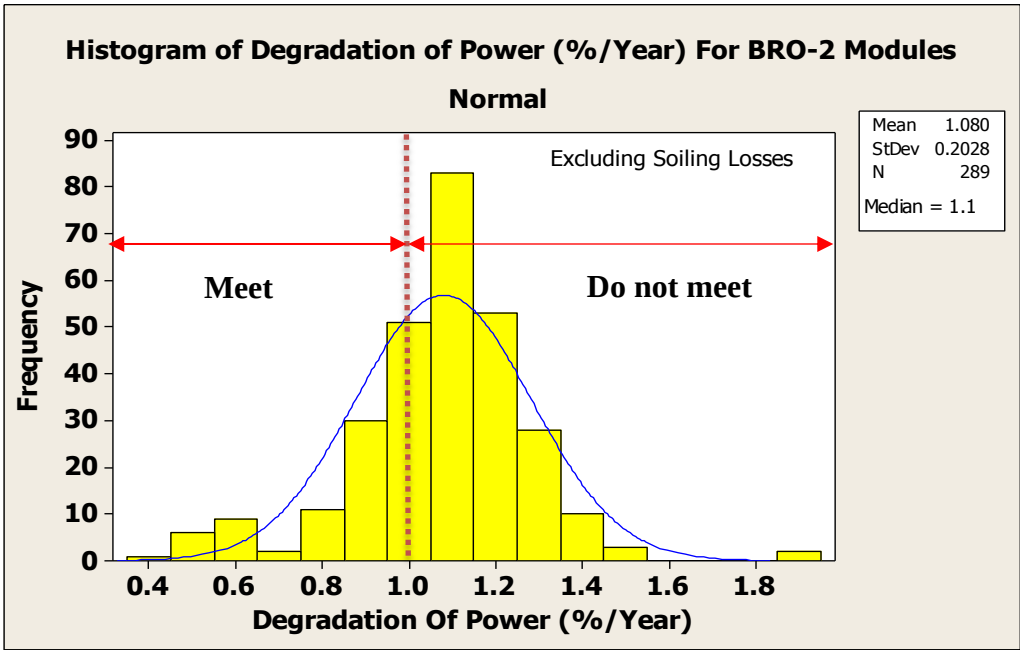

Figure 36 Histogram of Power Degradation (%/year) for all BRO 2 modules.

The plot shown in Figure 36 indicates a mean degradation rate of 1.08%/year and a median degradation rate of 1.1%/year.

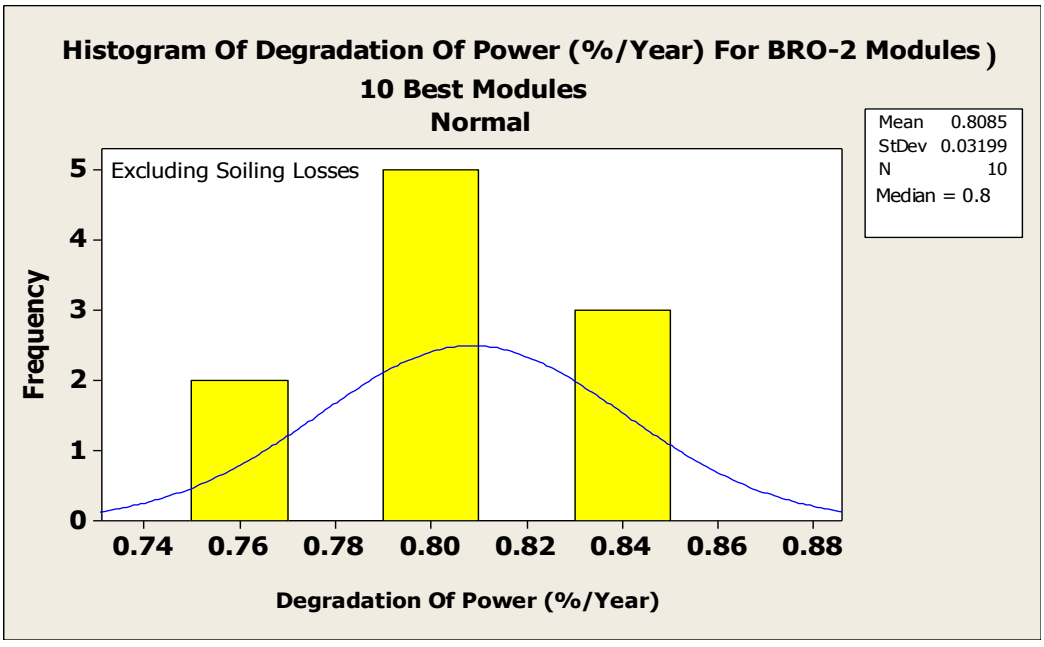

Figure 37 Histogram of Power Degradation (%/year) for 10 Best BRO 2 modules.

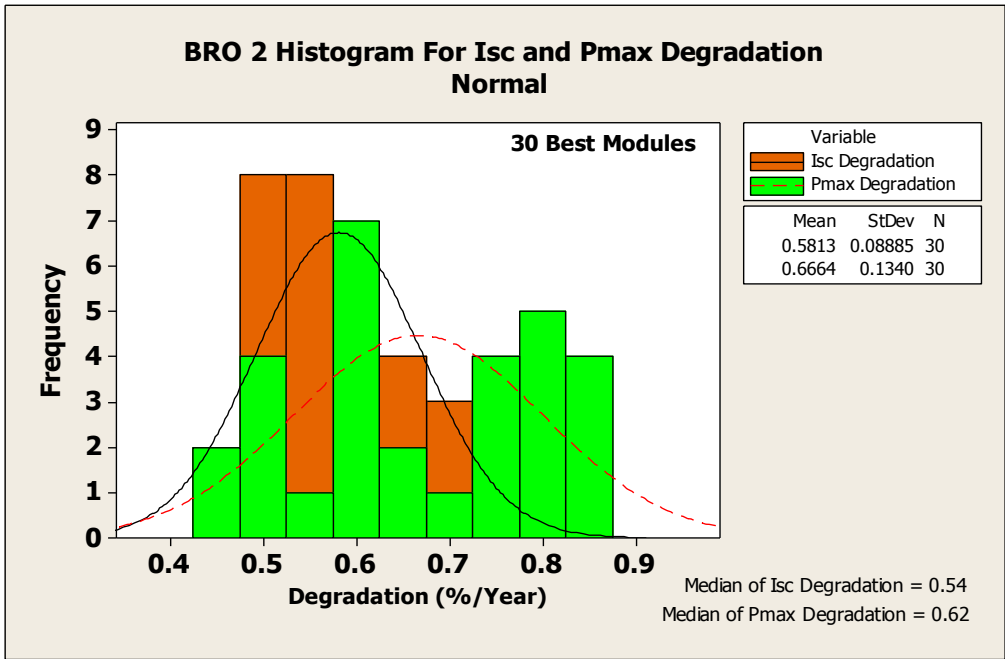

Figure 38 Histogram on Isc and Pmax degradation for 30 best modules in BRO 2

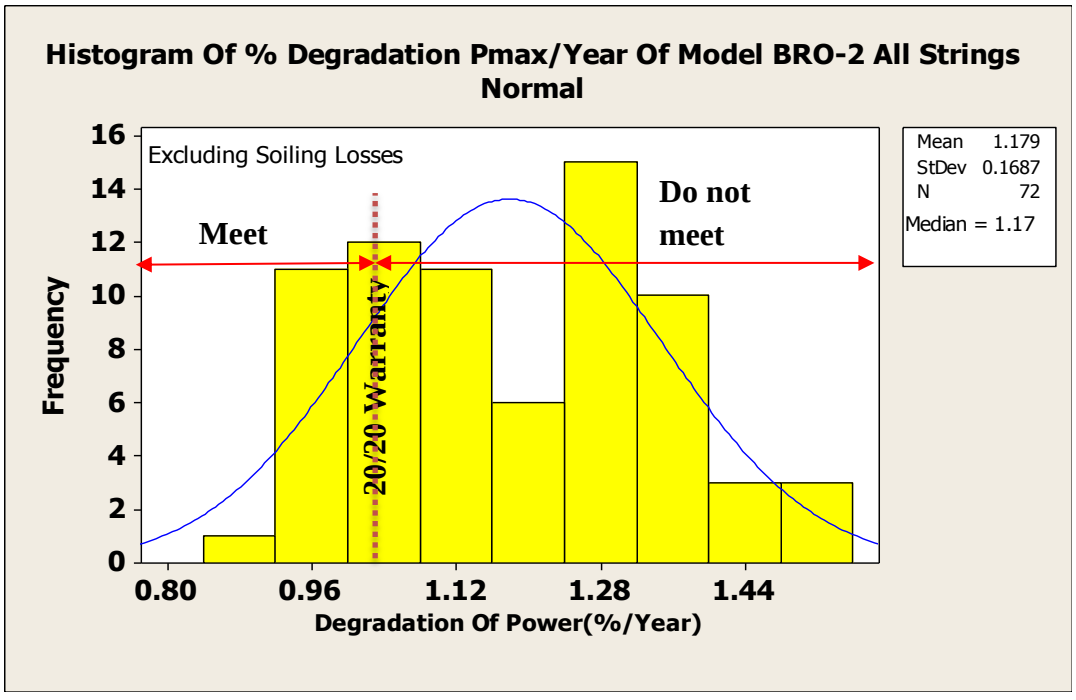

Figure 39 Histogram of Power Degradation (%/year) for all strings with BRO 2 modules

4.4 Visual Inspection

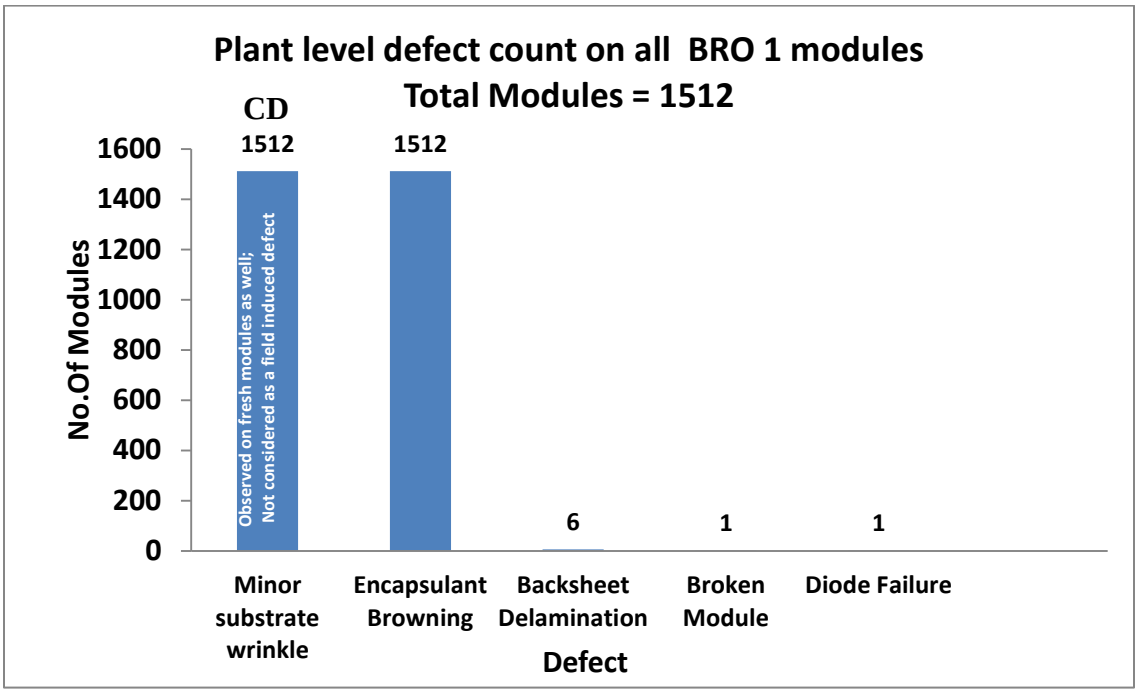

Figure 40 Bar graph on defects for all BRO 1 modules

4.4.1 Site 4A

The bar graph shown above in Figure 40 accounts for the defects recorded for Site 4A, all 756 modules have back sheet substrate warping between the J-box and the edge of the module and around the edges. This trend is typically seen in glass-polymer frameless modules because of the absence of a frame and thus a sealant between the back skin and the frame. Encapsulant browning covered 30-40% of every cell at the center on all modules. 6 modules had moderate to severe back sheet peel. Only 1 of 2 bypass diodes for a single module failed in the entire system.

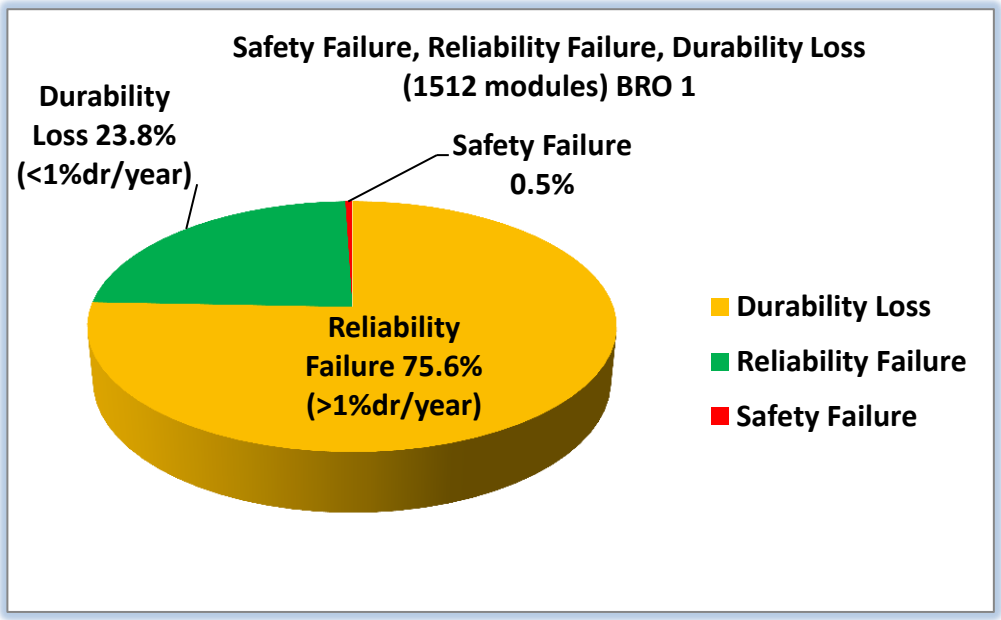

Figure 41 Durability loss, safety and reliability failure percentage for all modules in Site- 4A

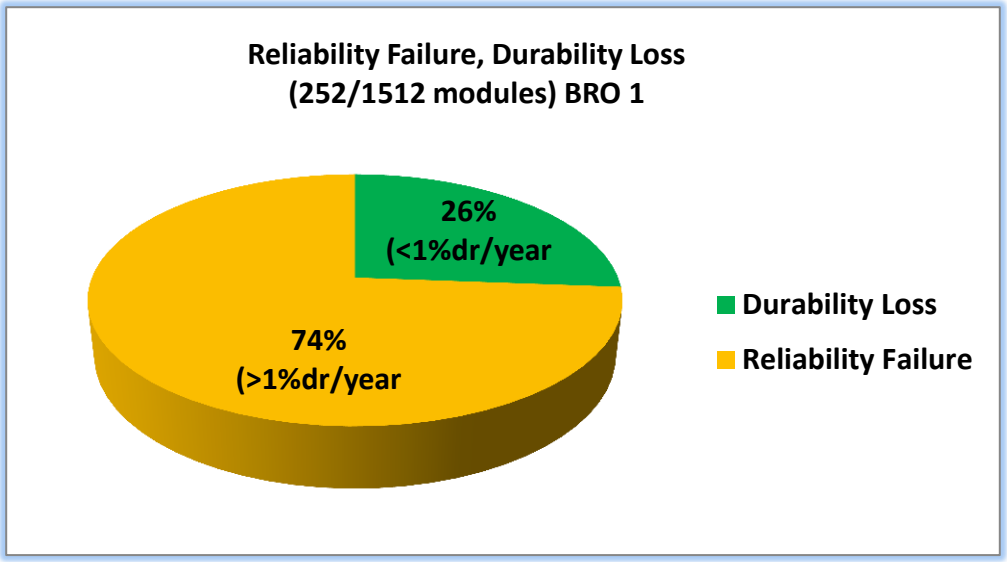

Figure 42 Reliability failure and Durability Loss site-4A

The pie chart in figure 42 indicates that 74% of the modules in Site 4A have a Pmax degradation rate of above 1%/year, this drop categorizes them under modules with reliability failures because they fail to meet the warranty terms. A vast percentage of

modules are in yellow region of the pie chart because of a combined effect of high series resistance due to solder bond fatigue and optical losses due to encapsulant browning. The 0.5% safety failure is due to one failed bypass diode, one broken module and 6 modules with back sheet delamination. The 26% of the total modules in the red region constitute durability loss because of only encapsulant browning and very low series resistance.

4.4.2 Site 4B

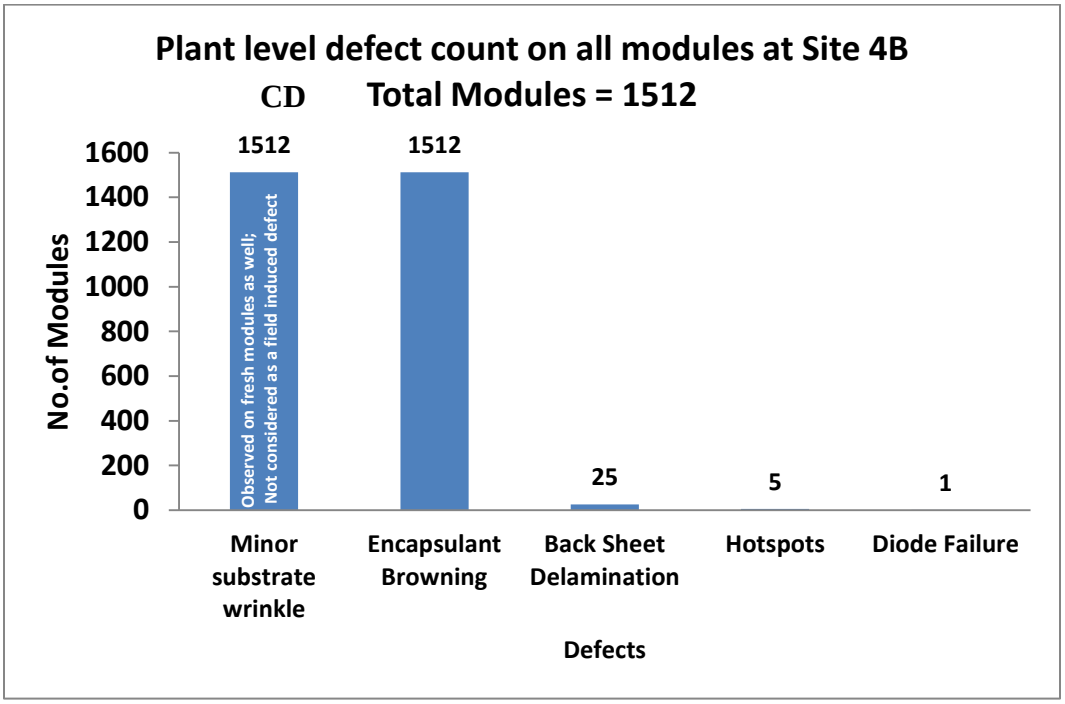

Figure 43 Bar graph on defects for all modules Site-4B.

The bar graph shown in

Figure 43 depicts results similar to that of Site 4A; except for the modules with hot spots, back sheet delamination and failure of only 1 of 2 bypass diodes for a single module in the entire system. The hotspots and diode failure account for less than 1% of the defects seen in Site 4B.

The pie charts in Figure 44 and Figure 45 indicate a durability loss and reliability failure percentage similar to that of modules in site 4A, but a higher safety failure percentage of 1.7 because of 5 modules with back sheet delamination and one bypass diode failure.

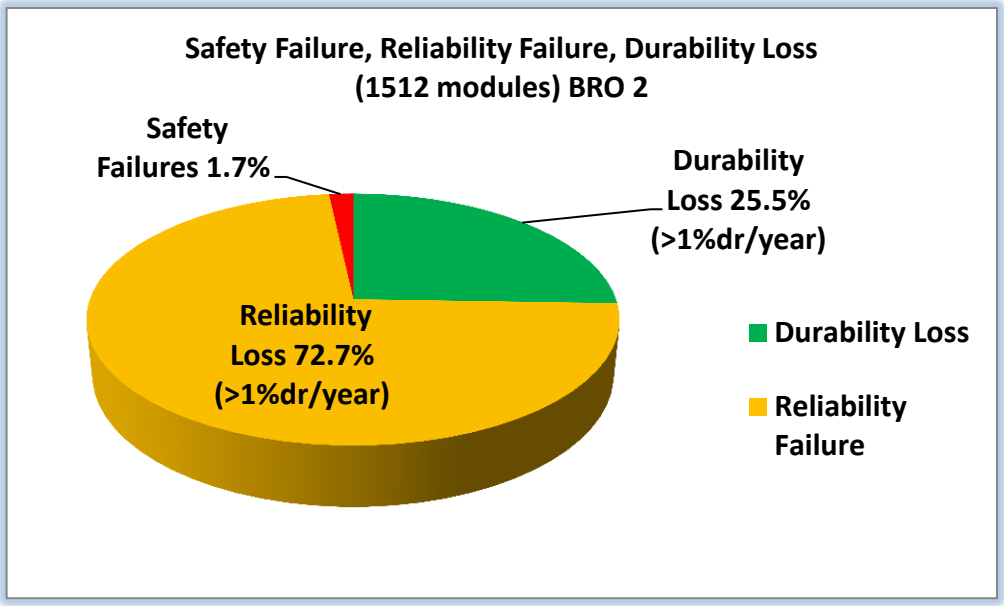

Figure 44 Durability loss, safety and reliability failure percentage for all modules in Site 4B

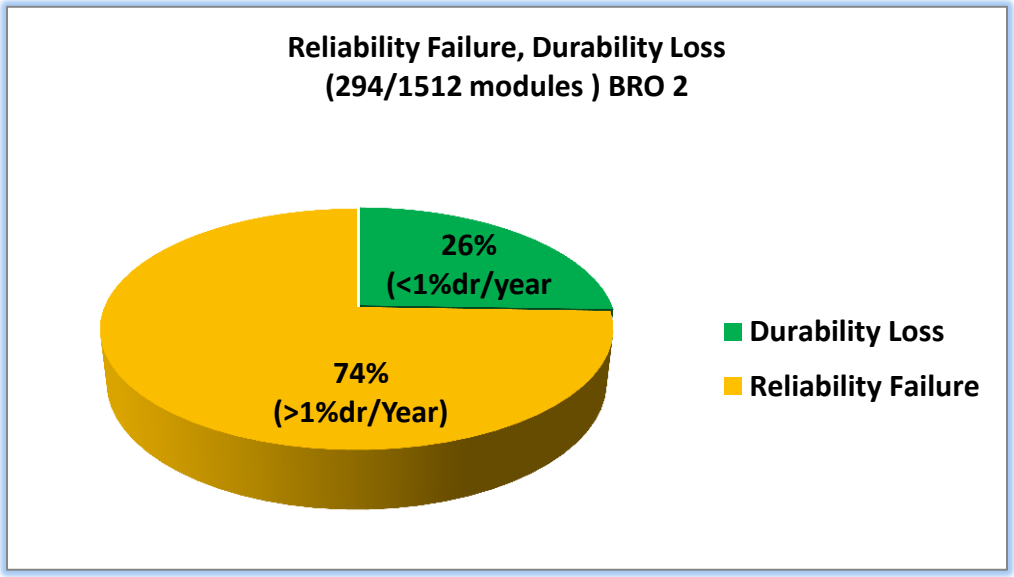

Figure 45 Reliability failure and Durability Loss site-4B

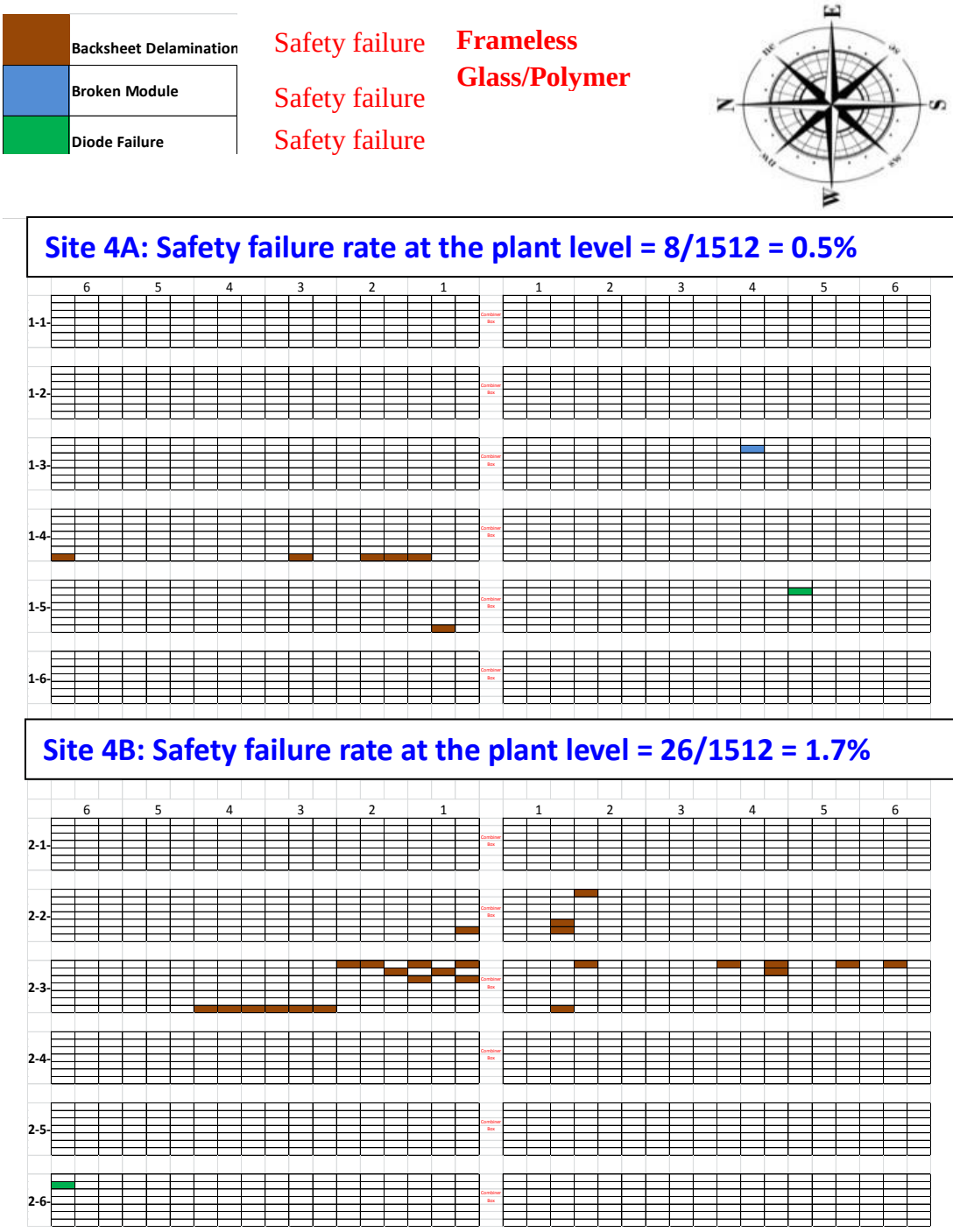

Figure 46 Safety Failure distribution In Site 4A&4B

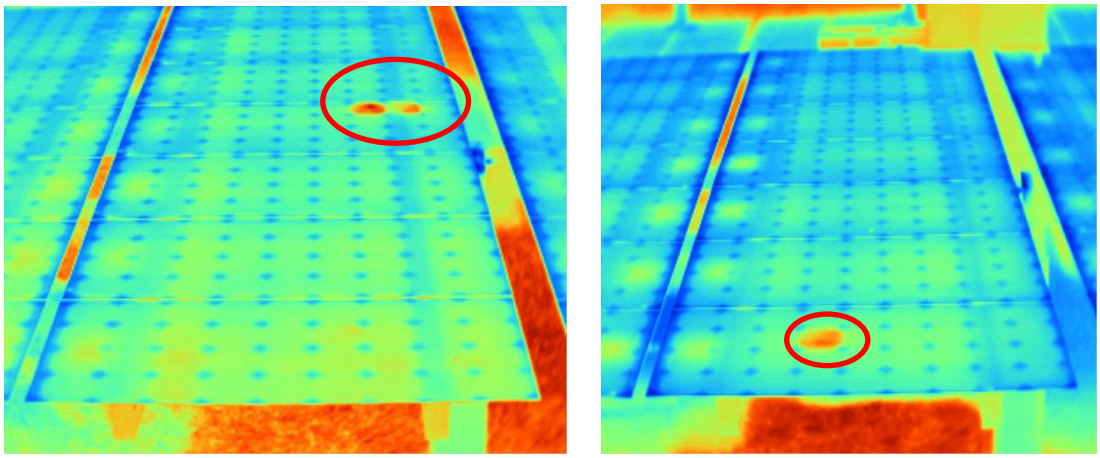

Figure 47 Hot Spots

The modules shown in Figure 47 have hot spots, but they were not severe enough to cause a burn through the back sheet, hence they were not considered as safety failures. The cell hot spots on two different modules the voltage drop caused in the diodes because of these hotspots is not adequate enough to trigger the bypass diode. The temperature differences of the cells with hotspots were between 7-10^{o} C when compared to the surrounding cells.

Table 9 Back sheet Delamination typically seen on the edges of frameless models.

	
	

The back sheet delamination shown in the images above have been considered as electrical safety hazards because the exposed surfaces can shock a person in the presence of moisture.

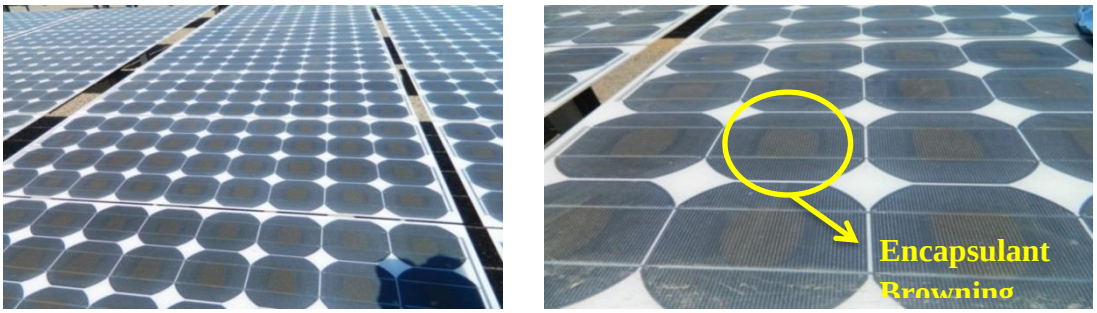

Figure 48 Encapsulant Browning

Figure 48 showing the significant amount of encapsulant browning on the cells that is affecting transmissivity of light. Browning occurs when UV rays begin to degrade the EVA. Eventually as the EVA degrades, it can form acetic acid that corrodes internal cell ribbons.

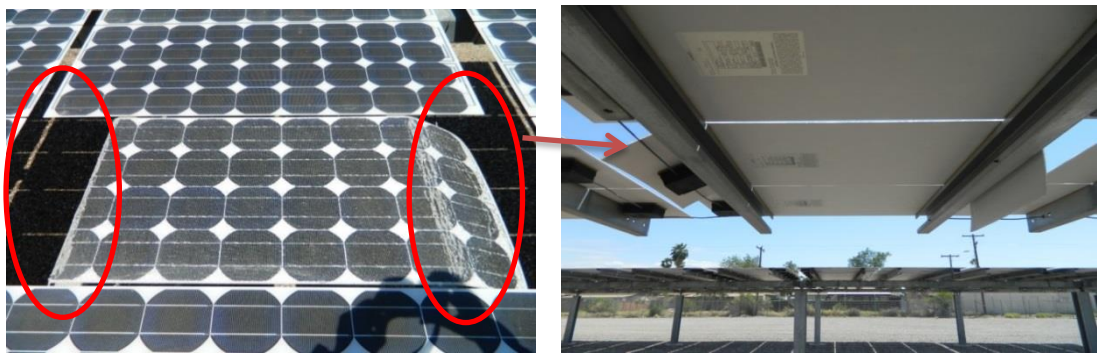

Figure 49 Broken Module in Site 4A

4.5 Potential Induced Degradation (PID)

Potential induced (PID) degradation is also responsible for durability issues in modules. The effect of voltage (PID) on the degradation of modules connected in a string was examined as well. PID occurs because numerous modules are connected in a string to achieve higher voltages. Three factors favored the absence of PID at the two evaluated plants, they are as follows:

1. Series connection of PV modules to obtain higher voltage levels in a power plant setting;
2. Positively biased strings throughout the power plant due to centralized negative grounding in the inverter.

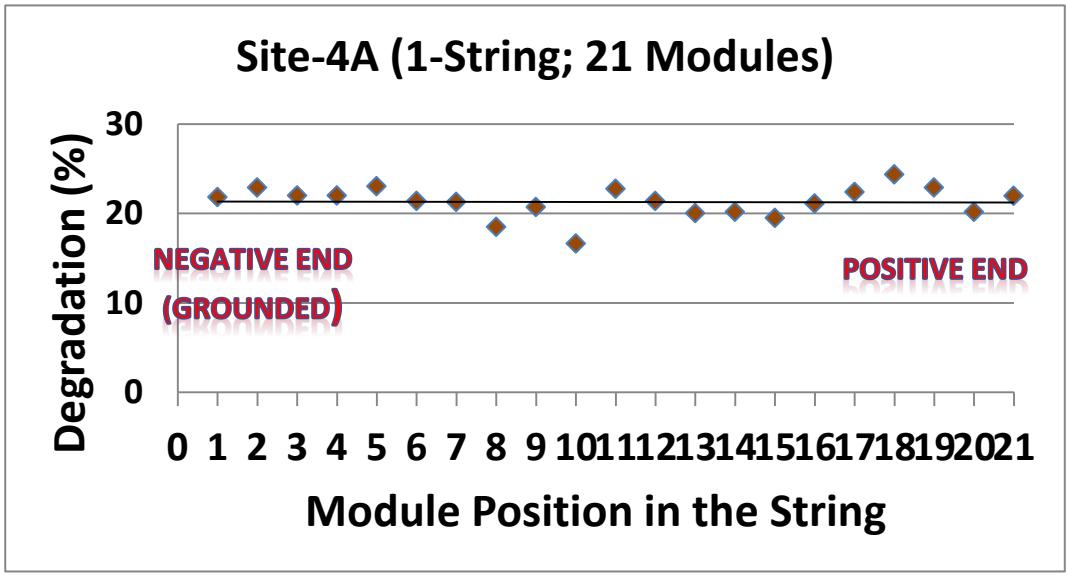

Figure 50 Absence of PID in Site 4A

From Figure 50 and Figure 51 these plots indicate that the modules haven't undergone any potential induced degradation due to high system voltages. A higher degradation rate was observed at the positive end.

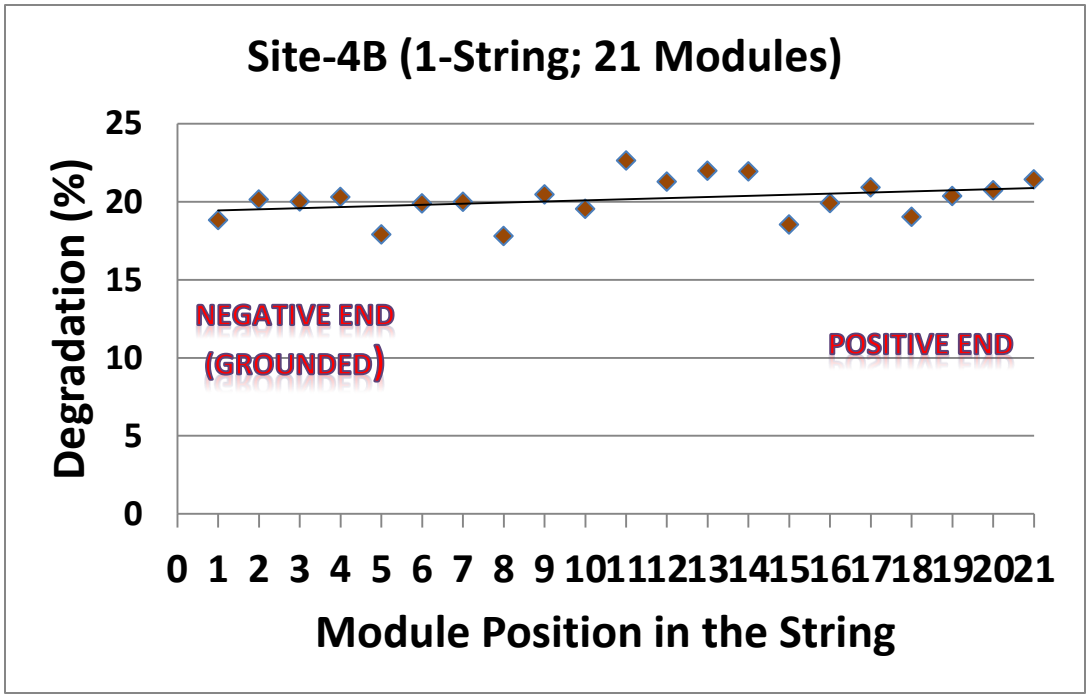

Figure 51 Absence of PID in Site 4B

4.6 Soiling Study

Excessive soiling and absence of frequent rains can cause a drop in performance. Soiling is a temporary and recoverable durability issue. It reduces the transmittance of the light onto the solar cells which lead to losses in Isc. String level IV curves were taken in a soiled state which was the state of operation of the power plant. These strings were then cleaned with water and dried before taking another set of IV curves. Thus, two string level IV curves were taken, one before and after cleaning. This action could not be

repeated for all the strings due to a time constraints and the height of the array above the ground.

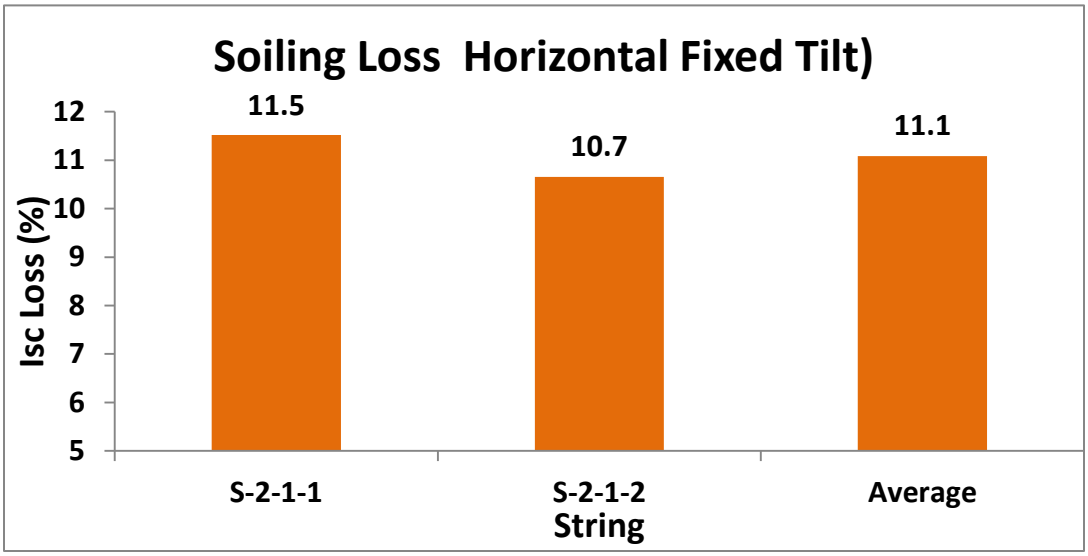

Figure 52 Soiling loss in site-4B

Figure 52 shows an average of 11.1% for the soiling losses in the two randomly selected strings. The difference between the measured soiled and cleaned Isc (string level) was taken in order to accurately obtain the Isc loss %.

4.7 Wind Effect On Durability

The modules performance is also dictated by the operating temperature .Wind flow helps keep the modules cool. The wind direction in and around Phoenix AZ is typically from the south –west. If there is a wind direction effect, the strings in the south-west are expected to degrade at lower rate than the north-east array because the circulation of air would affect the operating temperature of the arrays. As shown in Figure 53, there is approximately 35 feet distance between the Site-4A&4B site and the Site 4C site in the south and 15 feet between the Site-4A and Site-4B sites themselves. There is a minimum

80 foot clearance on both the east and the west side of the installation, which eliminates any effect the wind might have.

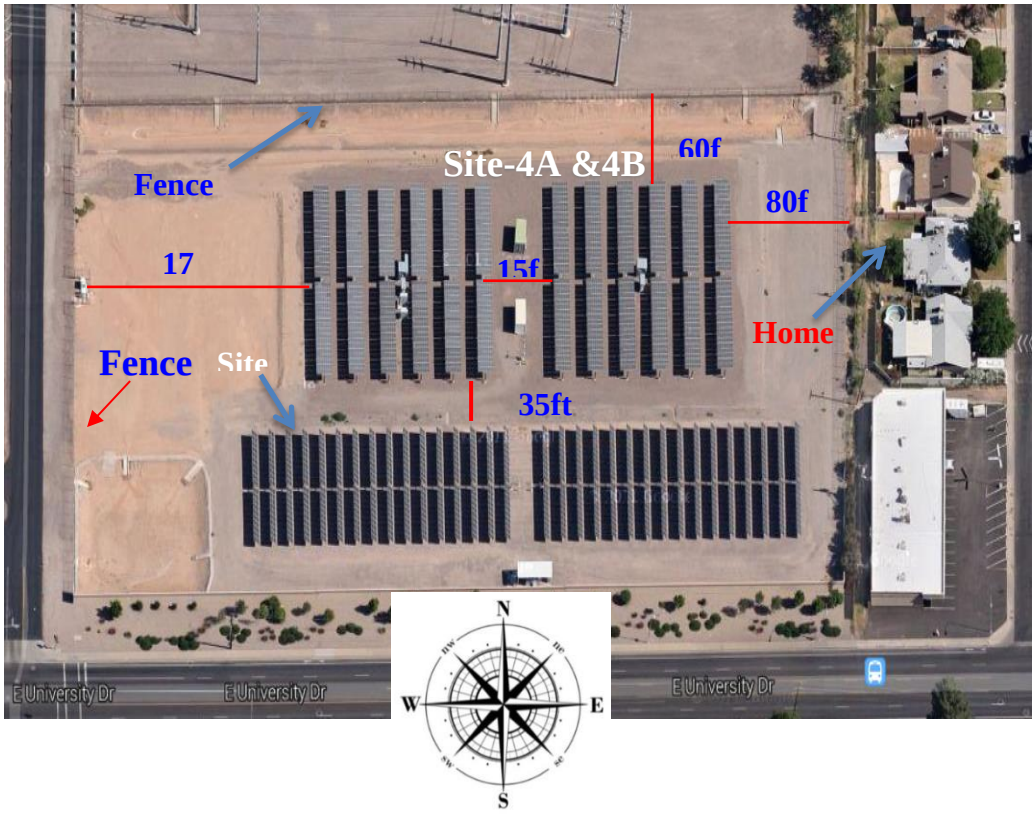

Figure 53 Site-4A &4B Google satellite image (approximate distances)

NORTH														SOUTH
		6	5	4	3	2	1	1	2	3	4	5	6	
	1-1	1263	1304	1301	1265	1276	1279	1305	1321	1230	1276	1294	1320	
	1-2	1254	1272	1263	1281	1240	1233	1262	1249	1258	1291	1283	1277	SYSTEM-1
	1-3	1251	1198	1221	1210	1211	1231	1206	1202	1292	1215	1211	1223	
				INVERTER						INVERTER				
	1-4	1195	1209	1219	1195	1201	1207	1228	1155	1191	1233	1251	1237	
	1-5	1198	1196	1170	1232	1179	1178	1230	1235	1248	1221	1227	1216	
	1-6	1239	1235	1206	1235	1228	1217	1242	1223	1221	1248	1254	1253	
				CONT-1						CONT-2				
	2-1	1208	1202	1218	1196	1180	1181	1256	1247	1175	1211	1181	1182	
	2-2	1307	1299	1291	1268	1281	1283	1169	1172	1179	1183	1189	1200	SYSTEM-2
	2-3	1302	1275	1303	1267	1250	1268	1220	1221	1288	1277	1280	1285	
				INVERTER						INVERTER				
	2-4	1228	1215	1212	1198	1206	1220	1299	1282	1288	1265	1261	1237	
	2-5	1234	1266	1266	1252	1241	1288	1306	1300	1308	1136	1243	1230	
	2-6	1324	1304	1301	1301	1289	1252	1251	1216	1207	1219	1213	1217	
NORTH		6	5	4	3	2	1	1	2	3	4	5	6	SOUTH

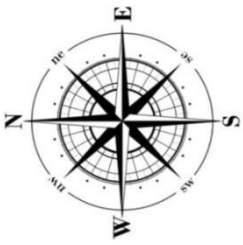

Figure 54 String Power Layout (Layout inverted to N-S orientation for spacing).

CHAPTER 5

CONCLUSION

5.1 Degradation Rates

Average degradation rate is 0.85%/year for the best modules and 1.1%/year for all the modules (excluding the safety failed modules). On an average of all the modules, the modules do not meet the typical 20/20 warranty expectations. Primary safety failure mode is the backsheet delamination though it is small (less than 1.7%). Primary degradation mode and reliability failure mode may potentially be attributed to encapsulant browning leading to transmittance/current loss and thermo-mechanical solder bond fatigue (cell-ribbon and ribbon-ribbon) leading to series resistance increase. Average soiling loss of horizontal tilt based modules is 11.1%. About 0.5-1.7% of the modules qualify for the safety returns under the typical 20/20 warranty terms, 73-76% of the modules qualify for the warranty claims under the typical 20/20 power warranty terms and 24-26% of the modules are meeting the typical 20/20 power warranty terms.

5.2 Encapsulant Browning and Series Resistance

Encapsulant browning was widely witnessed on almost all modules in both the systems. This observation was compared to the results of other reports on the same model and it was realized that this is a common problem with the modules from this design. Encapsulant browning is the primary contributor for drop in power in the best modules due to optical losses and a combination of browning and increase series resistance caused due to solder bond fatigue is the cause for power drop in the worst modules. Previous studies done on the same model reported a degradation rate of 1.5%/year, this was

because the system that was evaluated was on a 1-axis tracker [11] whereas the system evaluated in this study experienced lower degradation rate (about 1.1%/year) due to lower annual sunlight exposure rate (first 7 years exposure on a 1-axis tracker and the next 9 years exposure on a fixed horizontal tilted rack).

5.3 Potential Induced Degradation (PID)

PID does not seem to be responsible for the degradation of negative grounded systems in the hot-dry desert climatic condition of Gilbert/Mesa, Arizona.

5.4 Soiling Losses

Since all modules in both systems were installed on a fixed horizontal mounting structure, the soiling loss was found to be high (about 11%).

5.5 Wind Effect

Since both sites 4A and 4B were open in all directions with no wind obstruction a minimum distance of 80 feet on the north and the south side, no effect of wind direction was seen on the strings. However, this needs to be further verified with additional studies through onsite simultaneous module temperature monitoring at various locations of the power plant along with the weather parameters.

WORKS CITED

[1] M. D. Kempe, G. J. Jorgensen, K. M. Terwillinger, T. J. McMahon, C. E. Kennedy and T. T. Borrek, "Acetic acid production and glass transition concerns with ethylene-vinyl," p. 15, 2006.

[2] J. K. GovindaSamy TamizhMani, "Accelerated Lifetime Testing Of Photovoltaic Modules," Solar ABCS, 2013.

[3] S. Argo and G. J, "AIP conference proceedgings presentation on case histories of EVA encapsulant discoloration in fielded modules".

[4] S. Electronics, "AN3432 Application Note How to choose a bypass diode for a silicon panel junction box".

[5] C. Honsberg and S. Bowden , "PVCDROM," [Online]. Available: http://pveducation.org/pvcdrom.

[6] S. Kurtz and J. D.C*, "Photovoltaic Degradation Rates—an Analytical Review," p. 18, 13 October 2011.

[7] G. TamizhMani, *PRL PV powerplant evaluation layout,* 2013.

[8] A. A. Suleske, "Performance Degradation of Grid-Tied Photovoltaic Modules in a Desert Climatic Condition," 2010.

[9] SRP, "Fact Sheet".

[10] Photonics, 2010.

[11] J. Singh, "Investigation of 1,900 Individual Field Aged Photovoltaic Modules for Potential Induced Degradation (PID) in a Positive Biased Power Plant," 2011.

APPENDIX A

Site 4A &4B PLOTS FOR VARIOUS I-V PARAMETERS

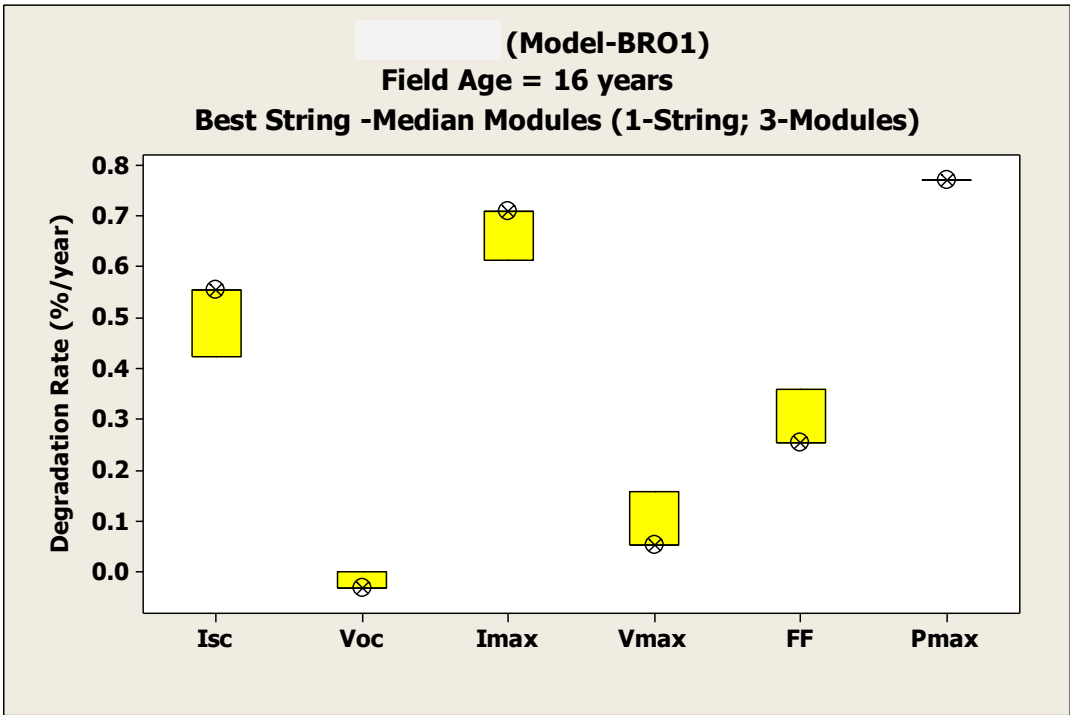

Figure A 1 BRO 1 Best String-Median Modules

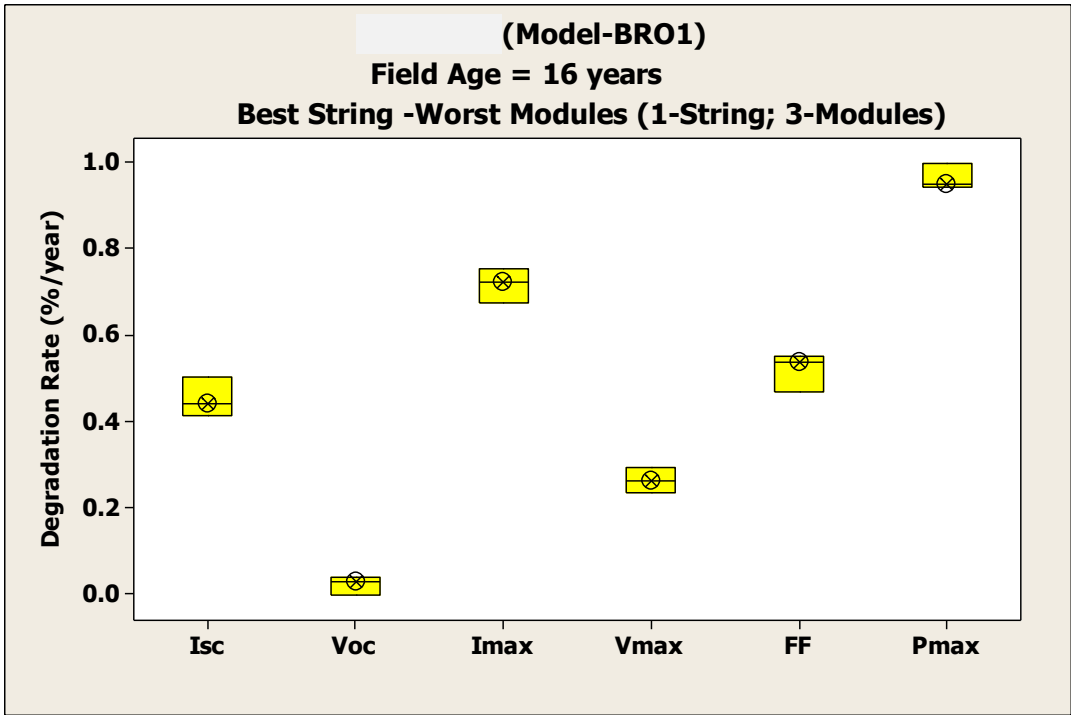

Figure A 2 BRO 1 Best String-Worst Modules

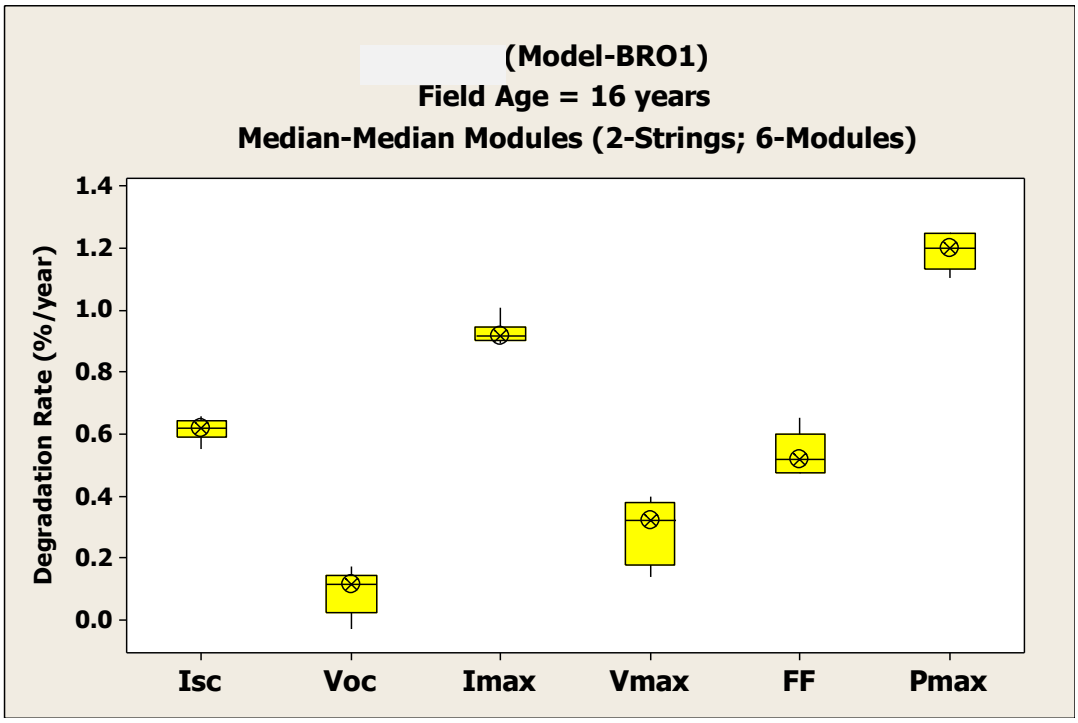

Figure A 4 BRO 1 Median String-Median Modules

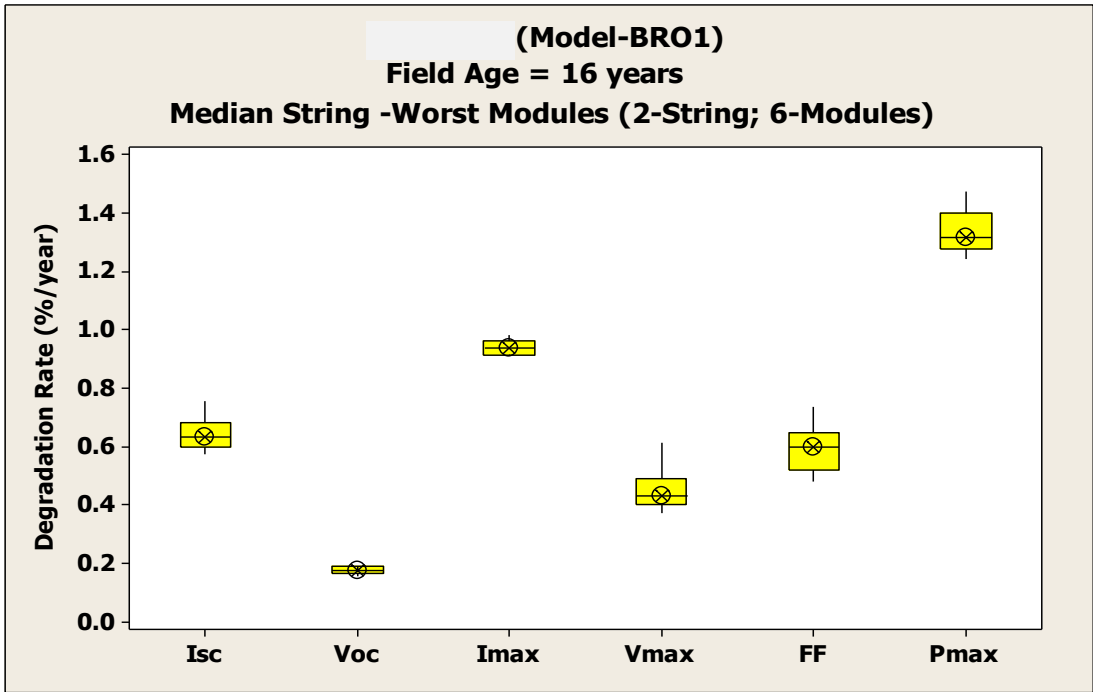

Figure A 4 BRO 1 Median String-Worst Modules

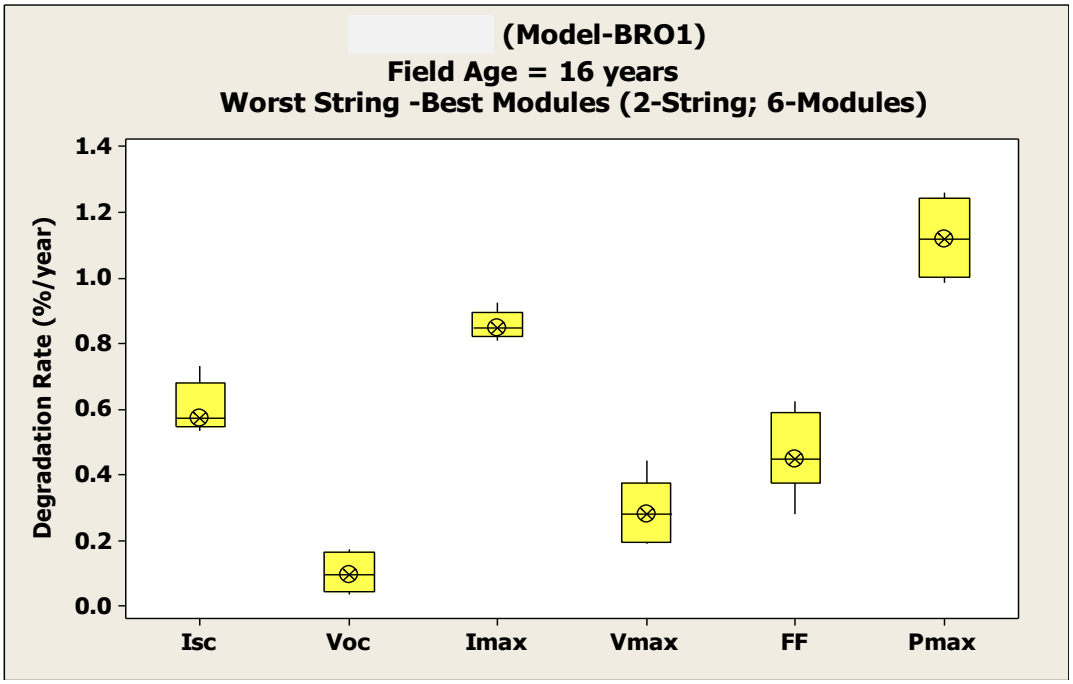

Figure A 6 BRO 1 Worst String-Best Modules

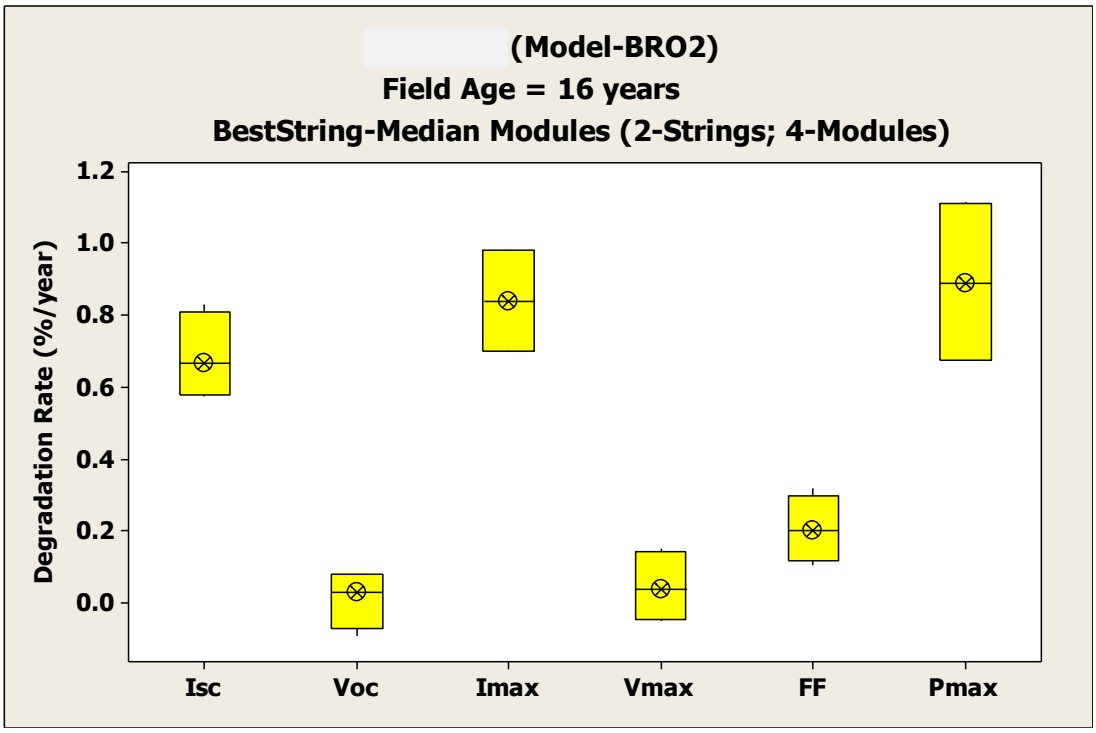

Figure A 5 BRO 2 Best String-Median Modules

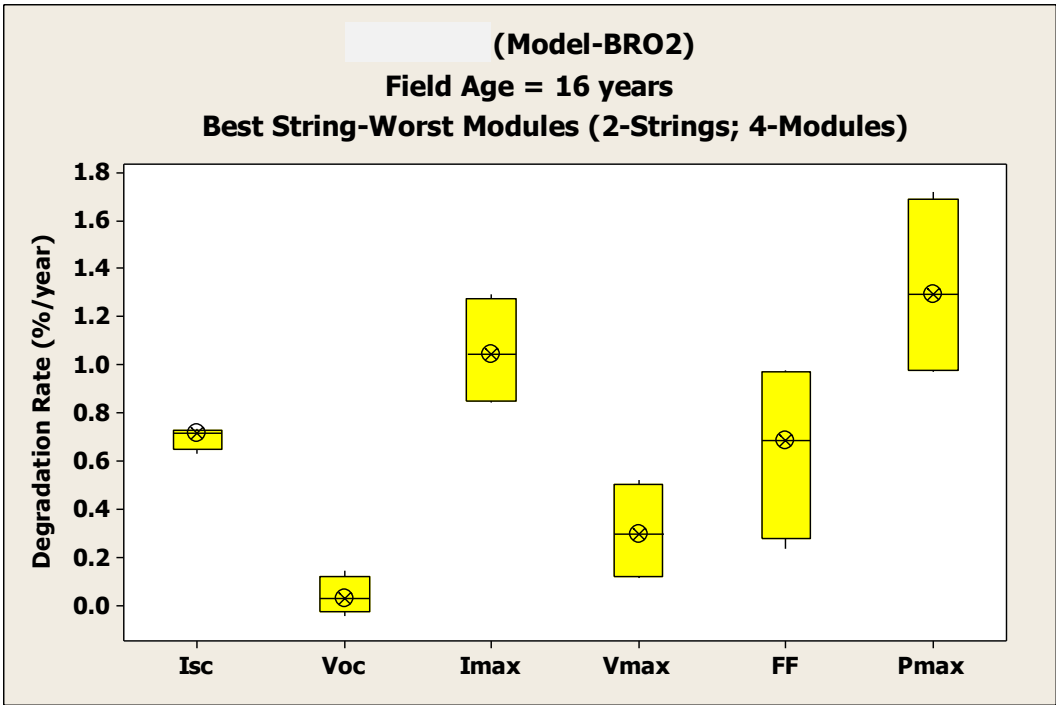

Figure A 8 BRO 2 Best String-Worst Modules

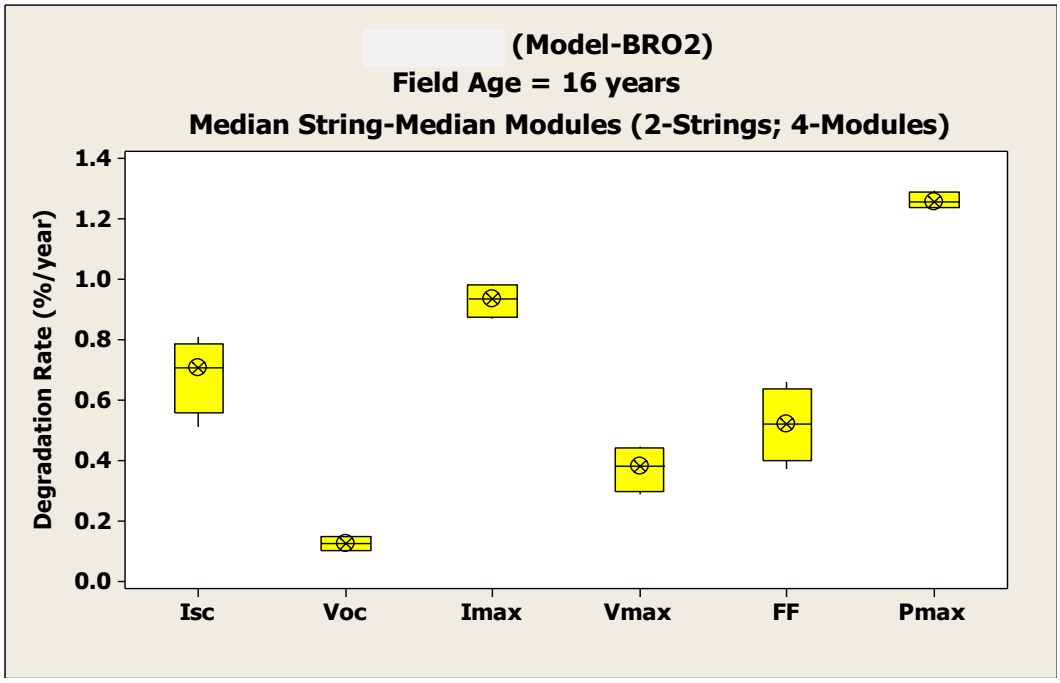

Figure A 7 BRO 2 Median String-Median Modules

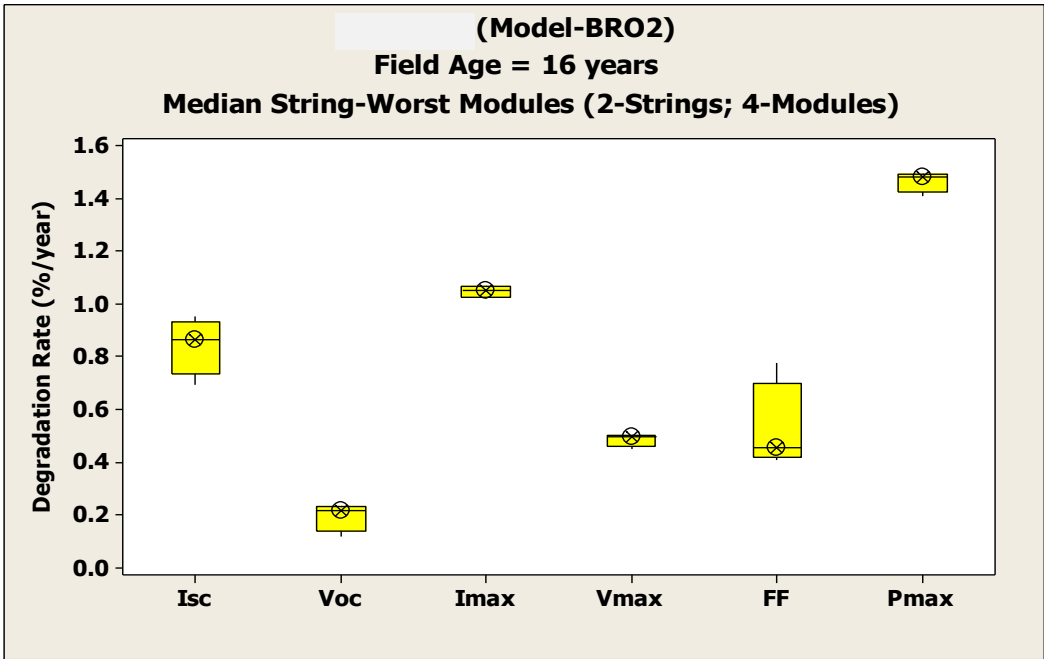

Figure A 10 BRO 2 Median String-Worst Modules

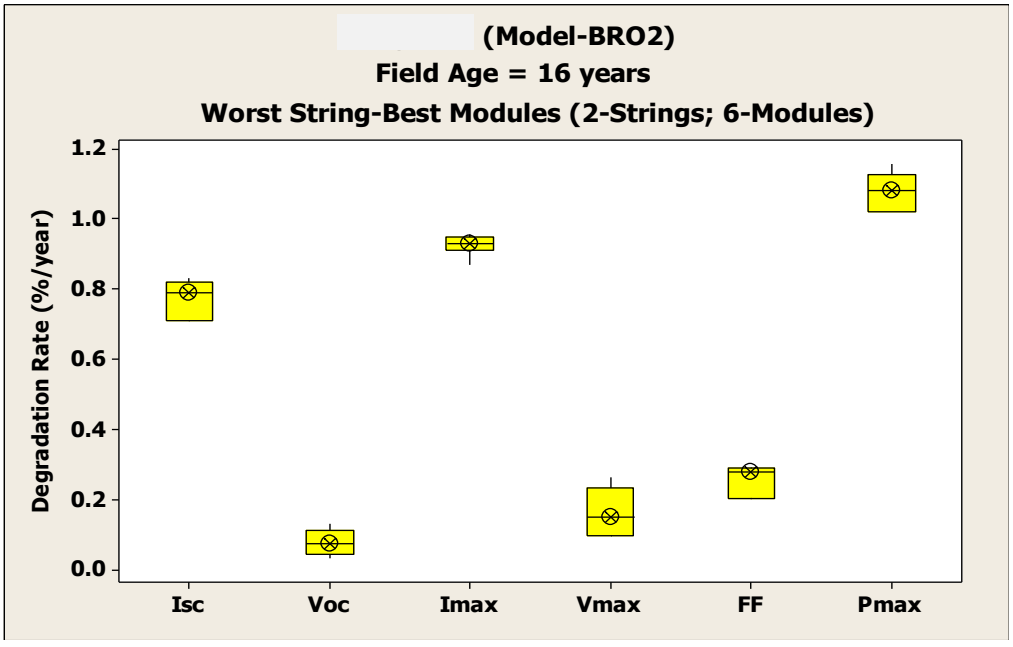

Figure A 9 BRO 2 Worst String-Best Modules